Characterization of the non-uniform geometry of mountain rivers

R.M. Hoeboer

April 1996

Preface

This report focuses on the project that I performed to conclude my Civil Engineering study at Delft University of Technology. The objective of the study is the characterization of the non-uniform geometry of a mountain river and the development of a method that identifies this geometry. Succeeding in identification of the geometry of a particular river section enables simplification in modelling. This is useful in wide range of applications, for example the prediction of water levels under flood wave conditions.

I wish to express my gratitude to my supervisors, prof. dr. ir. M. de Vries and dr. ir. Z.B. Wang, for their support and valuable comments. Highly appreciated are also the helpful discussions with ir. A. Sieben and the many suggestions he made.

R.M. Hoeboer
Delft, April 1996

Summary

Objective

The objective of the study is the characterization of the non-uniform geometry of a mountain river and the development of a method that identifies this geometry. Identification of the geometry enables simplification of a certain river section in modelling, which can be applied in a wide range of applications, for example the prediction of water levels.

Approach

Identification is based on the tracer methodology, which means that a non-disintegrating substance is released upstream of a river reach and water levels and concentrations are continuously measured. Therefore attention has been paid to the flow and transport processes in a mountain stream with irregular geometry.

The non-uniformity of the geometry of a mountain river affects the flow and transport processes. In the study the non-uniformity is modelled by the use of correction coefficients in the hydraulic model and the application of the stagnant zone concept in the transport model. The coefficients represent corrections for the influence of the non-uniformity of the depth and velocity profiles over the cross-section. The stagnant zone concept is based on the assumption of mass exchange between a zone with no net flow besides a main stream. A coupling can be found between the two concepts, which enables rewriting of the identified correction coefficients in a percentage of stagnant zones, relative to the total cross-section.

Based on those principles, a flow and transport simulating numerical model is developed. The applicability of the identification system is limited to streams with moderate Froude numbers. The determination of the parameters in a system, in this study the geometrical and hydraulic coefficients, is an identification problem. Integration of the numerical model with the parameter identification procedure DUD results in a system that identifies a geometry for which the produced observations of water levels and concentrations coincide with the measurements. An additional result is the reconstruction of the upstream, unsteady, discharge.

Conclusions

A river geometry and an upstream discharge can be identified yielding observations that coincide with the measurements. Besides values for the geometry-related parameters, values are identified for hydraulic and correction coefficients.

Test-cases verify the applicability of the identification system in two different situations. The system proved to be useful in a test-case that uses measurements based on instantaneous release of a tracer in a natural river under steady discharge conditions. The accuracy of the identification system was studied by means of 'synthetic' measurements, produced by numerical models. These measurements are based on continuous release of a tracer under flood wave conditions.

It is concluded that the system is well applicable for the identification of an unsteady discharge. Regarding the objective of the study some problems occurred. It turned out that the exactly 'true' geometry is never identified. Moreover, different combinations of parameter-values exist that produce, more or less, the same observations. This means that the uniqueness of the solution is questionable. While the accuracy of the identified geometry cannot be evaluated in the case of a natural river, one has to be cautious if the results are applied to simplify a river section.

Contents

1 Introduction

1.1 OBJECTIVE OF THE STUDY

After urbanization of low-land regions, the development of natural resources shifts to less-accessible areas. This has led to an increasing exploration of land and water in mountainous regions. Concerning river engaged projects in these regions, knowledge is required of the fluvial processes in the streams.

However, in contrast to low-land rivers, the description of the fluvial processes in mountain rivers is much more complicated. Mountain streams mostly have very irregular shapes, with big rocks, high turbulence, large Froude numbers and dead zones. Geometrical parameters such as depth, width, bottom slope and bottom roughness are time and place dependent. Flow velocities are distributed irregularly in the longitudinal direction, throughout each cross-section and in time. This means that, in the management of river engaged projects in mountainous regions, problems arise regarding a correct representation of the flow processes.

The objective of the study is the characterization of the non-uniform geometry of a mountain river and the development of a method that identifies this geometry. Identification of the geometry enables simplification of a certain river section in modelling, which can be applied in a wide range of applications, for example the prediction of water levels under flood wave conditions.

Identification of the geometry is based on the tracer methodology. Therefore attention has been paid to the theoretical and numerical description of flow and transport processes in mountain streams with a non-uniform geometry. A numerical flow and transport simulating model is developed. Integrated with a parameter identification procedure, the system identifies the geometry of a particular river section, merely based on measurements of water levels and concentrations. Based on several test-cases the applicability of the suggested method in natural mountain streams is discussed.

1.2 OUTLINE OF THE REPORT

Chapter 2 describes the principles that underlie the modelling of the non-uniformity of a mountain river: the use of correction coefficients and the stagnant zone concept. The method that is used to identify the irregular geometry, the dilution method, and preceding studies based on this method, are discussed.

In chapter 3 the basic equations describing the flow and transport processes in a mountain river are derived. The non-uniformity of the geometry affects phenomena of a propagating flood wave. Adjusted to the basic equations applied in this study, expressions are given for properties, such as the wave propagation speed and characteristic celerity.

Chapter 4 deals with the numerical aspects of the modelling. Numerical schemes are chosen to enable discretization of the basic equations. Properties of the schemes, such as numerical stability and accuracy, are discussed.

The parameter identification system is described in chapter 5. The system contains a flow and transport simulating model, based on the numerical approach discussed in chapter 4, and a parameter identification procedure, DUD. This procedure is used to find an optimal set of parameter-values describing the geometry of a mountain river. Because a numerical model can only be run if values for the system parameters are known, expressions are derived that can be used to find first order estimates of these values.

For a situation of continuous release of the tracer substance under flood wave conditions, the numerical identification system is tested in chapter 6. Using different sets of measurements, first the model is verified. Then cases are carried out to identify the geometry of a particular river section. Concluding remarks are made about the applicability of the identification system.

Finally, in chapter 7 a field case is discussed. Measurements are based on an instantaneous release of the tracer and are taken under steady discharge conditions, using a conductivity metre. Because the identification system discussed so far was based on measurements under unsteady discharge conditions, the method is slightly adapted. The numerical identified geometry is compared with the resulting geometry from an analytical approach.

Conclusions and recommendations are treated in chapter 8.

2 Principles of the study

2.1 THE DILUTION METHOD FOR DETERMINATION OF THE DISCHARGE

2.1.1 Steady flow

Observation of the dispersion of a dissolved tracer is a method used to determine a steady discharge. At an upstream point $x=0$ a tracer solution M (volume ΔQ) is introduced in a river at a constant rate (Fig.1). At the downstream point $x=L$ the concentration ϕ is measured. If M is released for a sufficiently long time, then at $x=L$ the equilibrium concentration ϕ_e is reached. If M and ϕ_0 (natural background concentration) are known then the discharge Q can be determined using the mass balance of the tracer. The method has been standardised (ISO, 1983) for a constant discharge Q.

$$Q = \frac{M - \Delta Q \phi_e}{\phi_e - \phi_0} \tag{2.1}$$

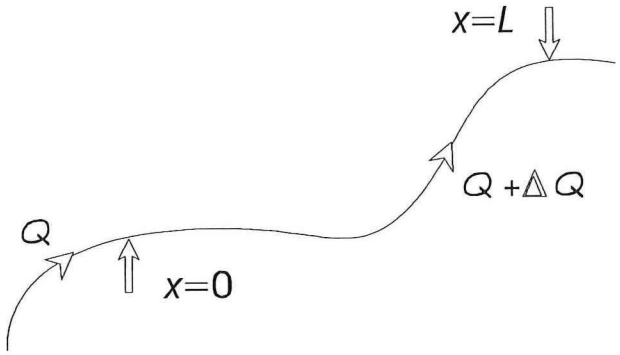

Fig.1 Dilution method

A simplified method is to use an NaCl-solution and a conductivity meter. Measurements obtained in this way are used in chapter 7. One condition is that the distance between the injection point and observation point (L) has to be sufficiently large to enable complete mixing to occur. Following minimum length is recommended:

$$L \geq 0.13 K \frac{B^2}{a} \tag{2.2}$$

Where the dimensionless dispersion coefficient K is given by:

$$K = \frac{C(0.7C + 2\sqrt{g})}{g} \tag{2.3}$$

It has been shown that this value for L is too pessimistic. Van Mazijk and de Vries (1990) proposed, on basis of the dispersion equations, that it is better to use:

$$L \geq 0.55 \frac{uB^2}{K_y} \tag{2.4}$$

in which K_y is the transversal dispersion coefficient, according to Fischer et. al. (1979).

$$K_y = 0{,}15au\frac{\sqrt{g}}{C} \tag{2.5}$$

2.1.2 Unsteady flow

Discharge measurements are especially interesting during flood wave conditions. Meijer (1992) showed the possibility to use the dilution method to determine an unsteady discharge, based on following data:

Continuous measurements of:

- $h(0,t)$: water level at $x=0$ [m]
- $h(L,t)$: water level at $x=L$ [m]
- $\phi(L,t)$: concentration at $x=L$ [kg/m^3]

Additional data:

- L : length of river section [m]
- ϕ_0 : background concentration for $x<0$ [kg/m^3]
- M : quantity of tracer release [kg/s]

A numerical model was developed that evaluated the measurements, estimated the river parameters and reconstructed the flood wave. If an upstream discharge and a set of river parameters were found that yielded results equal to the measurements, then one could have confidence in the determined river discharge.

2.2 APPROACH OF PRESENT STUDY

2.2.1 General

Due to high rates of turbulence relatively short mixing-lengths of transversal and vertical dispersion of injected solutes are exhibited in mountain streams. This adds to the applicability of the dilution method. However, it is now difficult to predict how the measured concentrations depend on the discharge. Longitudinal dispersion is a disturbing spreader of information and dead zones have a damping effect on the concentration cloud.

In the present study the dilution method is used to characterize the non-uniform geometry of a mountain stream. Based on the same data Meijer (1992) used, subsection 2.1.2, it is now the aim not only to identify the unsteady discharge but also values for parameters that characterize the irregular geometry of a mountain stream. Succeeding in this enables simplification of the geometry of a particular river section in modelling.

To enable indirect measurement of a geometry, a numerical flow and transport simulating model is developed, integrated with a parameter identification procedure. This system identifies a river geometry and an upstream unsteady discharge that yield observations of water levels and downstream concentrations that coincide with the measurements. The model is based on a coupling of a "transient-storage" model for the behaviour of the solute, and a hydraulic model corrected for the effects of a non-uniform geometry by introduction of correction coefficients. This means that, besides values for coefficients such as the width, roughness and bottom slope, values for additional coefficients have to be identified.

2.2.2 Use of correction coefficients

Simplification of the geometry of a river often results in a one-dimensional model, where cross-sectionally averaged values of the variables are used. This yields a correct representation of the flow processes when uniformity of the profiles is assumed. In the case of non-uniformity of the profiles, correction coefficients are introduced when the basic equations are integrated over the cross-section. The coefficients represent corrections for the fact that the product of mean values of variables is not equal to the mean of the product of these values (Jansen et. al., 1979).

Following variables are used in this study:

u	$= u(y,z)$	= time-averaged velocity in flow direction	[m/s]
a	$= a(y)$	= depth	[m]

The cross-sectionally averaged values of the variables are defined as

$$\bar{u} = \frac{\int_{y_l}^{y_r} u(y)\,dy}{B} \quad ; \quad u(y) = \frac{\int_{z_b}^{z_w} u(y,z)\,dz}{a(y)} \tag{2.6}$$

$$\bar{a} = \frac{\int_{y_l}^{y_r} a(y)\,dy}{B} \tag{2.7}$$

Where:

$z_w - z_b = a.$

$\bar{u}$ = cross-sectionally averaged value of velocity in flow direction [m/s]

$\bar{a}$ = mean depth of the flow [m]

While integration over the cross-section is carried out in two steps, the introduced coefficients are derived in two steps as well. The first step is a correction for the non-uniformity of the profiles over the depth, the second step results in correction over the total cross-sectional area. The definitions of the correction coefficients are given below.

A better understanding in which way these coefficients correct the non-uniformity can be gained by assuming a hypothetical distortion of the time mean value from the time and cross-sectionally mean value in each variable. Suppose:

$$u(y,z) = \bar{u} + \epsilon_u(y,z) \Rightarrow \overline{u(y,z)} = \bar{u} \quad ; \quad \overline{\epsilon_u(y,z)} \equiv 0 \tag{2.8}$$

$$a(y) = \bar{a} + \epsilon_a(y) \Rightarrow \overline{a(y)} = \bar{a} \quad ; \quad \overline{\epsilon_a(y)} \equiv 0 \tag{2.9}$$

The mean deviation is zero by definition. This yields the following expressions for the correction coefficients:

$$\alpha_u = \frac{\int_{y_l}^{y_r}\int_{z_b}^{z_w} u(y,z)\,dz\,dy}{\bar{u}\bar{a}B} = 1 + \frac{\overline{\epsilon_a \epsilon_u}}{\bar{a}\bar{u}} \tag{2.10}$$

$$\beta_u = \frac{\int_{y_l}^{y_r}\int_{z_b}^{z_w} u^2(y,z)\,dz\,dy}{\bar{u}^2 \bar{a} B} = 1 + \frac{2\overline{\epsilon_a \epsilon_u}}{\bar{a}\bar{u}} + \frac{\overline{\epsilon_u^2}}{\bar{u}^2} + \frac{\overline{\epsilon_u^2 \epsilon_a}}{\bar{u}^2 \bar{a}} \qquad (2.11)$$

β_u is called the *Momentum* or *Boussinesq coefficient.*

The correction coefficients are introduced in the model when the basic equations describing the flow processes are integrated over the cross-section in order to obtain a one-dimensional model. Additionally to the coefficients defined above, a correction coefficients β_a will occur in the equations due to integration over the cross-section. The definition will be given after introduction in the equations.

2.2.3 The stagnant zone concept

Stagnant zones, parts of the cross-section that do not carry any net flow, can be found in mountain rivers behind obstacles as boulders. Due to exchange of dissolved substance between the main flow and the stagnant zones the convective velocity of the dissolved matter becomes smaller than the mean flow velocity ($\bar{u}$). This causes a delay in the downstream arrival time and skewness in the observed downstream concentration curve (Fig.2). The effects are described by the distinction in the model of a storage width with zero mass-flux besides a main stream.

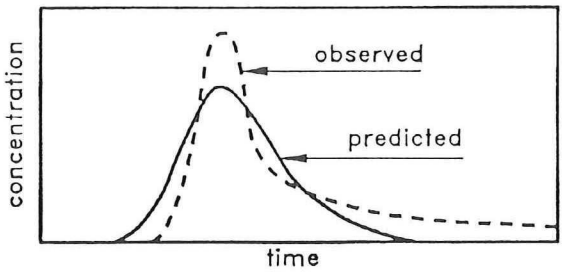

Fig.2 Difference between measured and predicted concentrations (Thackston and Schnelle, 1970)

Related to the total cross sectional area ($A=aB$) the portion of stagnant zones is $A_s=\beta_s \cdot A$, where β_s is the stagnant zone coefficient. The occurrence of these zones on the length of the river section (L) is defined by the fraction f. In the main stream zone (subscript *ms*), the variables are assumed to be uniformly distributed. In figure 3 the simplification of the geometry is schematized:

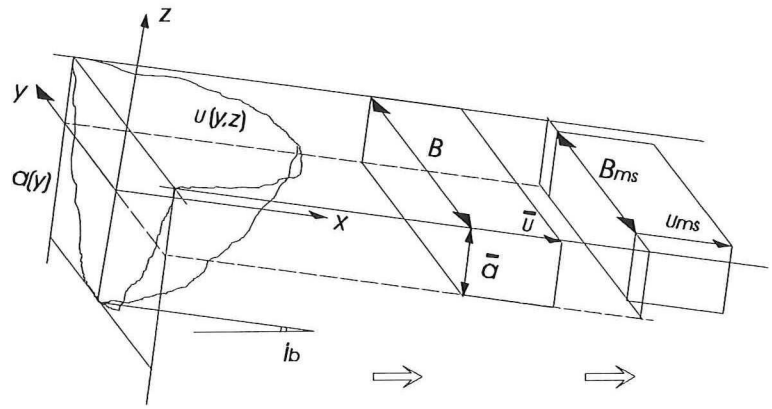

Fig.3 Coupling between stagnant zone concept and correction coefficients

The image in the middle represents the approach of introduction of the correction coefficients. The image on the right hand side represents the stagnant zone concept. The cross-sectional convection of mass and momentum is equal for the two approaches, which yields a coupling between the stagnant zone concept and the introduction of correction coefficients (Sieben, 1995):

$$u_{ms} a_{ms} (1-\beta_s) B = \alpha_u \bar{u} \bar{a} B \tag{2.12}$$

$$u_{ms}^2 a_{ms} (1-\beta_s) B = \beta_u \bar{u}^2 \bar{a} B \tag{2.13}$$

It is assumed that the depth in the main stream (a_{ms}) equals the mean depth ($\bar{a}$), which yields a relation between the use of correction coefficients and the stagnant zone concept:

$$u_{ms} = \frac{\beta_u}{\alpha_u} \bar{u} \tag{2.14}$$

$$\beta_s = 1 - \frac{\alpha_u^2}{\beta_u} = \frac{A_s}{A} \tag{2.15}$$

3 Flow and Transport processes

3.1 GENERAL

In transport processes the flowing water is the carrier of the transported substance. The water movement influences transport of the dissolved substance, but the dissolvant is assumed not to influence the water movement (no density currents).

In the next sections the flow and transport processes are described separately. Later on the processes are merged into a model describing transport processes in mountain rivers. The flow processes are described by the differential equations based on conservation of mass and momentum. The transport processes are described by the mass balances of the dissolved substance in the main stream and in the stagnant zone.

3.2 FLOW PROCESSES

3.2.1 Conservation of mass and momentum

- *Definitions*

In the co-ordinate system the x-axes is assumed parallel to the main flow direction. This means that the acceleration due to gravity has two components: g_x and g_z.

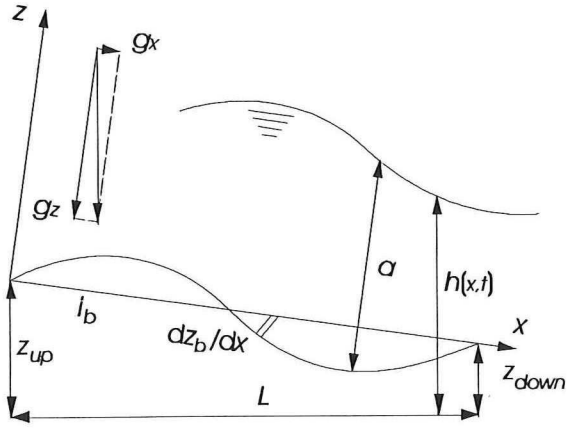

Fig.4 Definition sketch

In this turned co-ordinate system an average bottom slope i_b is introduced, given by:

$$i_b = \frac{z_{up} - z_{down}}{L} \tag{3.1}$$

In the horizontal plane the width of the river is allowed to be variable. Analogously to the definition of the average bottom slope, Eq. (3.1), a linear dependency of the width with the x-coordinate is introduced:

$$B(x) = B_0 + x\frac{B_{down} - B_{up}}{L} \tag{3.2}$$

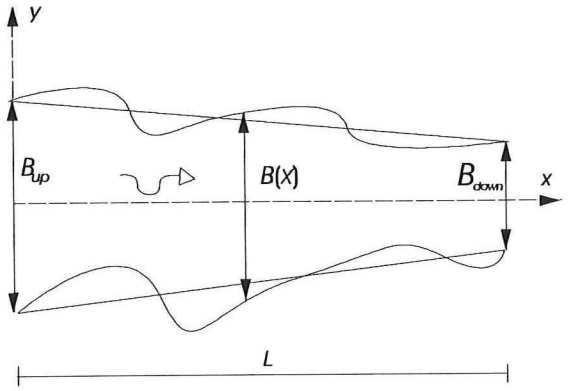

Fig.5 Variation in width

- *Basic equations*

Generally river flow is turbulent. This means that velocity components and pressure consist of a time-averaged part and a fluctuation caused by turbulence.

$$U = u + u'' \tag{3.3}$$

$$V = v + v'' \tag{3.4}$$

$$W = w + w'' \tag{3.5}$$

The equations describing the flow of the water are the equations of the conservation of mass and momentum. For a three dimensional model these equations are given by:

$$\frac{\partial u}{\partial x} + \frac{\partial v}{\partial y} + \frac{\partial w}{\partial z} = 0 \tag{3.6}$$

$$\frac{\partial u}{\partial t} + \frac{\partial (u^2)}{\partial x} + \frac{\partial (uv)}{\partial y} + \frac{\partial (uw)}{\partial z} + \frac{1}{\rho}\frac{\partial p}{\partial x} + \frac{1}{\rho}\frac{\partial \tau_{xy}}{\partial y} + \frac{1}{\rho}\frac{\partial \tau_{xz}}{\partial z} = g_x \tag{3.7}$$

$$\frac{\partial v}{\partial t} + \frac{\partial (uv)}{\partial x} + \frac{\partial (v^2)}{\partial y} + \frac{\partial (vw)}{\partial z} + \frac{1}{\rho}\frac{\partial \tau_{xy}}{\partial x} + \frac{1}{\rho}\frac{\partial p}{\partial y} + \frac{1}{\rho}\frac{\partial \tau_{yz}}{\partial z} = g_y \tag{3.8}$$

$$\frac{\partial w}{\partial t} + \frac{\partial (uw)}{\partial x} + \frac{\partial (vw)}{\partial y} + \frac{\partial (w^2)}{\partial z} + \frac{1}{\rho}\frac{\partial \tau_{xz}}{\partial x} + \frac{1}{\rho}\frac{\partial \tau_{yz}}{\partial y} + \frac{1}{\rho}\frac{\partial p}{\partial z} = g_z \tag{3.9}$$

Where:

U,V,W	= flow velocity components in x, y and z-direction	[m/s]
u,v,w	= time-averaged velocity-components in x, y and z-direction	[m/s]
u'',v'',w''	= turbulent flow velocity components in x, y and z-direction	[m/s]

The shear stresses are caused by turbulence and velocity gradients:

$$\tau_{xy} = \rho \overline{u''v''} - \rho \nu \frac{\partial u}{\partial y} = \rho \overline{u''v''} - \rho \nu \frac{\partial v}{\partial x} \tag{3.10}$$

$$\tau_{xz} = \rho \overline{u''w''} - \rho \nu \frac{\partial u}{\partial z} = \rho \overline{u''w''} - \rho \nu \frac{\partial w}{\partial x} \tag{3.11}$$

$$\tau_{yz} = \rho \overline{v''w''} - \rho \nu \frac{\partial v}{\partial z} = \rho \overline{v''w''} - \rho \nu \frac{\partial w}{\partial y} \tag{3.12}$$

Where:

ν	= kinematic viscosity of the water	[m^2/s]
$\tau_{i,j}$	= shear stress in i,j-plane	[N/m^2]

3.2.2 Integration over the cross section

In order to obtain a one-dimensional flow model that uses cross-sectionally averaged values, the equations of motion have to be integrated over the cross section. Assuming that the influence of the local velocities v and w is included in the shear stresses, integration over the cross-section of equations (3.6) and (3.7):

$$\frac{\partial \bar{a}B}{\partial t} + \frac{\partial \alpha_u \bar{u}\bar{a}B}{\partial x} = 0 \tag{3.13}$$

$$\frac{\partial \alpha_u \bar{u}\bar{a}B}{\partial t} + \frac{\partial \beta_u \overline{u^2}\bar{a}B}{\partial x} + \frac{1}{\rho}\int_A\int \frac{\partial p}{\partial x}\,dy\,dz + \frac{1}{\rho}\int_A\int \frac{\partial \tau_{xy}}{\partial y}\,dy\,dz + \frac{1}{\rho}\int_A\int \frac{\partial \tau_{xz}}{\partial z}\,dy\,dz = g_x \tag{3.14}$$

We notice that, due to integration over the cross-section, the correction coefficients representing the non-uniform distribution of the velocity and the depth profiles over the cross-section (subsection 2.2.2) are introduced in the equations. The four last terms of (3.14) are analysed separately.

The pressure p is assumed to consist of a hydrostatic pressure distribution and a fluctuation due to turbulence:

$$p = \rho g_z (a + z_b - z) + p'' \tag{3.15}$$

This means that *the third term* of (3.14) can be rewritten:

$$\frac{1}{\rho}\int_A\int \frac{\partial p}{\partial x}\,dy\,dz = \frac{1}{2} g_z \beta_a \frac{\partial \overline{a^2}B}{\partial x} + g_z \bar{a}B\frac{\partial z_b}{\partial x} + \frac{1}{\rho}\frac{\partial}{\partial x}\left(\overline{p''}\bar{a}B\right) \tag{3.16}$$

The correction coefficient β_a is defined analogously to the definitions presented in subsection 2.2.2, where ϵ_a is defined as the deviation of the depth from the mean value $\bar{a}$. This coefficient represents the non-uniformity of the depth profile over the cross-section.

$$\beta_a = \frac{\int_{y_l}^{y_r} a^2(y)\,dy}{\bar{a}^2 B} = 1 + \frac{\overline{\epsilon_a^2}}{\bar{a}^2} \tag{3.17}$$

It is obvious that $\beta_a \geq 1$. Hereafter the *overbars* over the cross-sectionally averaged values will be omitted as no unaveraged quantities will be used.

The difference between the two hydrostatic forces on the cross-sections $x=x$ and $x=x+dx$ is compensated by the forces on the water of the inclining bottom and of the deviation in width. This last force can be defined as:

$$-g_z\beta_a\frac{a^2}{2}\frac{\partial B}{\partial x} \tag{3.18}$$

The influence of a variable width on the resulting pressure is counterbalanced by the borders themselves (pressure of the borders on the water equals the pressure of the water on the borders, due to variation in width). This can be shown by the first term on the right hand side of equations (3.16) and (3.18):

$$\frac{1}{2}g_z\beta_a\frac{\partial a^2 B}{\partial x} - g_z\beta_a\frac{a^2}{2}\frac{\partial B}{\partial x} = g_z\beta_a aB\frac{\partial a}{\partial x} \tag{3.19}$$

It is now assumed that the last term of (3.16), due to pressure fluctuations, equals zero. When the average bottom slope i_b is used, $dz_b/dx=0$ and therefore the third term of (3.16) equals zero as well.

The fourth and fifth term of equation (3.14) can be rewritten into:

$$\frac{1}{\rho}\int_A\int\left(\frac{\partial\tau_{xy}}{\partial y} + \frac{\partial\tau_{xz}}{\partial z}\right)dy\,dz = \frac{P\tau_b}{\rho} \approx \frac{\tau_b(1-\beta_s)B}{\rho} \tag{3.20}$$

Where:

P	= wetted perimeter	[m]
τ_b	= mean bottom stress	[N/m^2]

Integration of *the term on the right hand side* of the momentum equation yields:

$$\int_A\int g_x = g_x aB = g_z i_b aB \tag{3.21}$$

Because the effect of a non-uniform geometry is described with the stagnant zone concept, a term has to be added to the equation of momentum that accounts for the exchange of momentum between main stream and stagnant zone:

$$fEu_{ms}^2 a \tag{3.22}$$

Where:

f	= fraction of stagnant zones relative to river section length L	[-]
E	= entrainment coefficient	[-]

The resulting system of equations describing the water movement:

$$\frac{\partial aB}{\partial t} + \frac{\partial \alpha_u uaB}{\partial x} = 0 \tag{3.23}$$

$$\frac{\partial \alpha_u uaB}{\partial t} + \frac{\partial \beta_u u^2 aB}{\partial x} + g_z \beta_a aB \frac{\partial a}{\partial x} = g_z i_b aB - \frac{\tau_b (1-\beta_s)B}{\rho} - fEu_{ms}^2 a_{ms} \tag{3.24}$$

We notice that, of the terms representing production of momentum with opposite sign, the resistance due to bottom stress (equation 3.20) is proportional to the main stream width $(1-\beta_s)\cdot B$. The momentum exchange represented by (3.22) on the other hand is proportional to the contact length of the stagnant zone and the main stream, approximately a, and to the velocity difference between main stream and stagnant zone (u_{ms}- 0 = u_{ms}).

The resulting equations can be written as a system with A and Q as the dependent variables, defined as:

$$A = aB \tag{3.25}$$

$$Q = \alpha_u uaB \tag{3.26}$$

Under following assumptions the last two terms of (3.24) can be rewritten:
- constant Chézy parameter representing the bottom roughness
- uniform velocity distribution (assumed in main stream zone)
- prismatic channel (assumed in main stream zone).

$$\begin{aligned} -\frac{\tau_b (1-\beta_s)B}{\rho} &= -\frac{g_z}{C^2} u_{ms}^2 (1-\beta_s)B = \\ &= -\frac{g_z}{C^2}\frac{\beta_u^2}{\alpha_u^4}(1-\beta_s)\frac{Q^2}{A^2}B = -\frac{g_z}{C^2}\sigma_u \frac{Q^2}{A^2}B \end{aligned} \tag{3.27}$$

$$-fEu_{ms}^2 a = -fE\frac{\beta_u^2}{\alpha_u^4}\frac{Q^2}{AB} = -fE\sigma_u^2\frac{Q^2}{AB} \tag{3.28}$$

For the sake of simplicity of the equations a coefficient σ_u has been defined:

$$\sigma_u = \frac{\beta_u}{\alpha_u^2} = \frac{1}{1-\beta_s} = \frac{A}{A-A_s} \tag{3.29}$$

Notice that this coefficient represents the coupling between the modelling of non-uniform effects by means of correction coefficients, and the stagnant zone concept. The terms (3.27), frictional effects and (3.28), momentum exchange, are together responsible for the total energy dissipation:

$$\left(\frac{g_z}{C^2}\frac{B}{\sigma_u}+fE\frac{A}{B}\right)\sigma_u^2\frac{Q^2}{A^2} \tag{3.30}$$

Finally the following equations of continuity and momentum are found describing the flow processes:

$$\frac{\partial A}{\partial t}+\frac{\partial Q}{\partial x}=0 \tag{3.31}$$

$$\frac{\partial Q}{\partial t}+\sigma_u\frac{\partial}{\partial x}\left(\frac{Q^2}{A}\right)+g_z\beta_a A\frac{\partial}{\partial x}\left(\frac{A}{B}\right)=g_x A-\frac{g_z}{C^2}\sigma_u\frac{Q^2}{A^2}B-fE\sigma_u^2\frac{Q^2}{AB} \tag{3.32}$$

3.2.3 Comments on the resulting flow equations

The momentum equation presented above slightly differs from the momentum equation that can be found in, for example, Jansen et al. (1979). Apart from the introduction of two components of the gravitation constant, due to turning of the co-ordinate system, the appearance of an extra term and additional coefficients is obvious. The last term of equation (3.32) is additional compared to the traditional momentum equation and represents, as explained before, the momentum exchange between main stream and stagnant zones.

The additional coefficient β_a is a correction coefficients which corrects the influence of the non-uniformity of the depth over the width. The coefficient σ_u represents the coupling between the use of correction coefficients and the stagnant zone concept Eq. (3.29). This means that the identified value for σ_u corrects the flow processes for the presence of dead zones and for the effects of non-uniform distribution of the flow-velocity in main stream direction over the cross-sectional area. This coefficient can be compared with the coefficient α' that is introduced in Jansen et al., in this respect that than α_u (Eq. 2.10) equals one by definition.

Values for the correction coefficients can be found by measuring the velocity and the depth profiles. The method discussed in this study provides in indirect identification of values for the parameters and coefficients of the hydraulic equations.

Appendix A gives two examples of hypothetical depth and velocity profiles with the coefficients σ_u and β_a to match. The image is merely taken up for illustrative reasons. The value of the stagnant zone coefficient β_s is calculated from the value of σ_u, which illustrates the possibility to express corrections for the non-uniformity of the profiles in a geometrical coefficient.

3.3 WAVE PROPAGATION PHENOMENA

3.3.1 General

Equations (3.31) and (3.32) describe the flow processes in a mountain river. Because the non-uniformity of the geometry is described by the use of correction coefficients and the stagnant zone concept, additional coefficients are introduced in the equations (f, E,σ_u and β_a). To show the influence of the introduced coefficients on the flow processes, some wave propagation phenomena, valid in this study, are derived below. Some of the results will be used further in the study (section 5.2).

3.3.2 Critical flow

In steady flow the time derivatives are omitted from the continuity equation (3.31) and from the equation of momentum (3.32). In this case an expression can be found for the backwater curve:

$$\frac{\partial A}{\partial x} = \frac{g_x A - \frac{g_z}{C^2}\sigma_u \frac{Q^2}{A^2} B - fE\sigma_u{}^2 \frac{Q^2}{AB}}{g_z \beta_a \frac{A}{B} - \sigma_u \frac{Q^2}{A^2}} \tag{3.33}$$

From this expression it can be concluded that the slope of the water surface becomes infinite if

$$\frac{\sigma_u \left(\frac{Q^2}{A^2}\right)}{g_z \beta_a \left(\frac{A}{B}\right)} = 1 \tag{3.34}$$

Or, using equations (3.25), (3.26) and (3.29)

$$\frac{\beta_u}{\beta_a}\frac{u^2}{g_z a} = \frac{\beta_u}{\beta_a} F_r^2 = 1 \tag{3.35}$$

This means that critical flow occurs for $F_r^2 = \beta_a/\beta_u$, where $F_r^2 = u^2/(g_z a)$.

3.3.3 Characteristic celerities

The physical meaning of the characteristic celerities is the propagation speed of infinite small disturbances at the water surface. Assuming a uniform width, the momentum equation (3.32) is rewritten to be able to find these celerities:

$$\frac{\partial Q}{\partial t} + 2\sigma_u \frac{Q}{A}\frac{\partial Q}{\partial x} + \left(g_z \beta_a \frac{A}{B} - \sigma_u \frac{Q^2}{A^2}\right)\frac{\partial A}{\partial x} = R \qquad (3.36)$$

Where R is the right-hand side of equation (3.32). Also the equations of the total differentials are available:

$$\mathrm{d}t\frac{\partial Q}{\partial t} + \mathrm{d}x\frac{\partial Q}{\partial x} = \mathrm{d}Q \qquad (3.37)$$

$$\mathrm{d}t\frac{\partial A}{\partial t} + \mathrm{d}x\frac{\partial A}{\partial x} = \mathrm{d}A \qquad (3.38)$$

Hence four equations are available which are linear in the partial derivatives: The continuity equation (3.31), the momentum equation (3.32) and the equations (3.37) and (3.38).

For small disturbances the derivatives are different at both sides of the disturbance. In other words the system of equations must allow two solutions for partial derivatives. Because the system of equations is linear it allows only one solution unless the system becomes indeterminate. This is the case if the determinant of the system matrix becomes zero:

$$\begin{vmatrix} 0 & 1 & 1 & 0 \\ 1 & 2\sigma_u Q/A & 0 & g_z\beta_a A/B - \sigma_u Q^2/A^2 \\ \mathrm{d}t & \mathrm{d}x & 0 & 0 \\ 0 & 0 & \mathrm{d}t & \mathrm{d}x \end{vmatrix} = 0 \qquad (3.39)$$

Given the definition $c = \mathrm{d}x/\mathrm{d}t$ this gives for the celerities:

$$c_{1,2} = \sigma_u \frac{Q}{A} \pm \sqrt{g_z \beta_a \frac{A}{B} + \frac{Q^2}{A^2}(\sigma_u^2 - \sigma_u)} \qquad (3.40)$$

Or, using again equations (3.25), (3.26) and (3.29)

$$\frac{c_{1,2}}{u} = \frac{\beta_u}{\alpha_u} \pm \sqrt{\frac{\beta_a}{F_r^2} + \beta_u\left(\frac{\beta_u}{\alpha_u^2} - 1\right)} \Rightarrow c_{1,2} = u_{ms} \pm \sqrt{g_z \beta_a a + \beta_s u_{ms}^2} \qquad (3.41)$$

In flow with uniformly distributed variables (α_u=1, β_u=1 and β_a=1) and stagnant zone coefficient β_s=0, the defined parameter σ_u=1 (3.29). In this case the expression of the propagation velocity (3.40) simplifies into:

$$c_{1,2} = \frac{Q}{A} \pm \sqrt{\frac{g_z A}{B}} = u \pm \sqrt{g_z a} \qquad (3.42)$$

Now three possibilities occur, using the results of subsection 3.3.2:

subcritical flow ($F_r^2 < \beta_a/\beta_u$):	one positive and one negative value for c
critical flow ($F_r^2 = \beta_a/\beta_u$):	c_1=0; c_2=2u;
supercritical flow ($F_r^2 > \beta_a/\beta_u$):	both values for c are positive.

The celerities are the slopes of the lines in the x,t-plane. Along these characteristic lines information propagates. This means that in the case of subcritical flow, supposed in this study, information can as well travel upstream as downstream. This imposes restrictions on the boundary conditions: as well an upstream as a downstream boundary-condition has to be given.

We can conclude that correction coefficients affect the behaviour of the flood waves. There is a shift of the point on which critical flow occurs and an adaption of the expression of the propagation speed.

3.3.4 Classification of long waves

In rivers most kind of waves, except wind waves, can be considered to be long. In long waves a characteristic length, for example the wave length, is much larger than the depth.

Theoretical considerations on long waves are based on the relevance of the friction term in the momentum equation. Two approaches are considered in which the frictional effects are either predominating, or negligible with respect to the inertial effects. For an estimation of the relevance of the friction term we use the following approach

$$u = u_{max}\cos(\omega t) \quad ; \quad \omega = \frac{2\pi}{T} \qquad (3.43)$$

In this way the relevance of the frictional effects with respect to the inertial effects is represented by Ω and depends on the flood wave period T:

$$\Omega = \frac{g_z u_{max}}{C^2 \omega a} \tag{3.44}$$

3.3.5 Inertia predominating friction

These kind of waves, in which the inertia is predominating the friction ($\Omega \ll 1$), are called seiches. Typical features of these waves are a relatively small wave period (T is in the order of ten minutes) and a small amplitude of the water level compared to the depth of the stream. When convective acceleration ($F_r < 1$) and frictional effects are neglected and a constant width is assumed, the system of equations simplifies into:

$$\frac{\partial A}{\partial t} + \frac{\partial Q}{\partial x} = 0 \tag{3.45}$$

$$\frac{\partial Q}{\partial t} + g_z \beta_a \frac{A}{B} \frac{\partial A}{\partial x} = 0 \tag{3.46}$$

Differentiating Eq. (3.45) with respect to t and Eq. (3.46) with respect to x enables elimination of Q or A. This yields two second order differential equations in x and t which are called the chord-equations.

$$\frac{\partial^2 A}{\partial t^2} - \frac{g_z \beta_a A}{B} \frac{\partial^2 A}{\partial x^2} = 0 \quad \Rightarrow \quad A = A_1(x + ct) + A_2(x - ct) \tag{3.47}$$

$$\frac{\partial^2 Q}{\partial t^2} - \frac{g_z \beta_a A}{B} \frac{\partial^2 Q}{\partial x^2} = 0 \quad \Rightarrow \quad Q = Q_1(x + ct) + Q_2(x - ct) \tag{3.48}$$

The solution consists of two components, (A_1,Q_1) and (A_2,Q_2), which are defined by conditions on the two spatial boundary's of the computational domain. As explained in subsection 3.3.3, because $F_r < 1$, one of the components propagates in the negative, the other in the positive x-direction, both with a celerity c Eq. (3.40).

In this approach the propagation velocity of the wave equals the propagation speed of small disturbances in the water surface. Examples of this kind of waves can be found in bores, low translatory waves, which can develop when emptying a lock-chamber.

3.3.6 Friction predominating inertia

Examples of these kind of waves in which the friction is dominant (Ω, Eq. (3.44) $\gg$ 1) can be found in flood waves on rivers. A typical time-scale for the wave period T is $4*10^3$ minutes, in which the water surface in one point of the river gradually rises and drops. Three approaches will be dealt with.

- *Dynamic wave model:*

This model is called dynamic because inertia is still taken into account. Solving the problem is based on the non-simplified momentum equation. Reasons why the inertia is not neglected can be found in faster propagating disturbances, superposed on the flood wave. Also on the upstream river reach of tropical rivers (banjirs) the inertia cannot be neglected in the flood wave itself.

- *Kinematic approach:*

The phenomena are so slow that inertial effects can be neglected. If the flow is considered quasi-steady and uniform, the surface slope is approached by the bottom slope, or

$$\left|\frac{\partial a}{\partial x}\right| \ll i_b \tag{3.49}$$

The momentum equation reduces to:

$$g_z i_b A - \frac{g_z \sigma_u}{C^2}\frac{Q^2}{A^2}B = 0 \tag{3.50}$$

In this case the depth adjusts itself to the discharge according to the rating curve. In this study this algebraic expression is given by:

$$Q = \frac{A}{\sqrt{\sigma_u}} C\sqrt{i_b a} \tag{3.51}$$

Only the continuity equation remains as differential equation, and represents the kinematic relations. Substitution of Eq. (3.51) in the continuity equation results in

$$\frac{\partial a}{\partial t} + c\frac{\partial a}{\partial x} + \frac{Q}{B^2}\frac{\partial B}{\partial x} = 0 \tag{3.52}$$

Where

$$c = \frac{3}{2}\frac{u}{\sqrt{\sigma_u}} \qquad ; \quad u = C\sqrt{i_b a} \tag{3.53}$$

In this approximation no wave attenuation occurs and the influence of the flood wave propagates slowly, compared to translatory waves. But, because the flow velocity u is a function of the depth a, there will be transformation of the wave. In higher parts of the wave u and, according to (3.53), also the propagation speed c will be larger.

- *Diffusion analogy:*

If the damping is important the surface slope has to be included in the momentum equation (Jansen et al.,1979). When the inertial effects are neglected, the flow is considered quasi-steady but non-uniform. The momentum equation reduces into an equilibrium equation, in which inertial effects counterbalance the force of the surface slope. It follows that

$$Q = \frac{A}{\sqrt{\sigma_u}} C\sqrt{a\left(i_b - \beta_a \frac{\partial a}{\partial x}\right)} \tag{3.54}$$

Substitution in the continuity equation yields an equation of the parabolic or diffusive type

$$\frac{\partial a}{\partial t} + c\frac{\partial a}{\partial x} - D\frac{\partial^2 a}{\partial x^2} + \frac{Q}{B^2}\frac{\partial B}{\partial x} = 0 \tag{3.55}$$

Where:

$$c = \frac{3}{2}\frac{u}{\sqrt{\sigma_u}} \qquad ; \quad u = C\sqrt{a\left(i_b - \beta_a \frac{\partial a}{\partial x}\right)} \tag{3.56}$$

and

$$D = \frac{C^2 \beta_a}{\sigma_u}\frac{a^3 B}{2Q} \tag{3.57}$$

The third term of Eq. (3.55) represents the diffusion and causes damping.

For both the kinematic and the diffusion approach, the propagation velocity can be rewritten in terms of the stagnant zone coefficient β_s, which yields:

$$c = \frac{3}{2} u \sqrt{1-\beta_s} \tag{3.58}$$

This shows that a delay in the arrival time of the concentration cloud appears when a stagnant zone is present.

It must be understood that fast surface waves (c represented by Eq. (3.40)) propagate continuously from each point of the flood wave. However these waves are damped by the predominating frictional term and the result is a slow wave, propagating with a velocity c Eq. (3.56).

The difference between the kinematic approach and the diffusion analogy can be shown by means of the 'hysteresis effect'. If the water surface slope is taken into account (diffusion analogy), then there are two possible values for the discharge for only one value of the depth. A consequence is that, during the passage of a flood wave, first the discharge and then the depth takes it maximum value. The rating curve is transformed into a loop. The relationship between Q and a is described by the Jones formula, obtained from Eq. (3.54):

$$Q = Q_s \sqrt{1 + \frac{\beta_a}{i_b c} \frac{\partial a}{\partial t}} \tag{3.59}$$

Where Q_s is the rating curve for steady flow Eq. (3.51). The figure below shows the hysteresis effect.

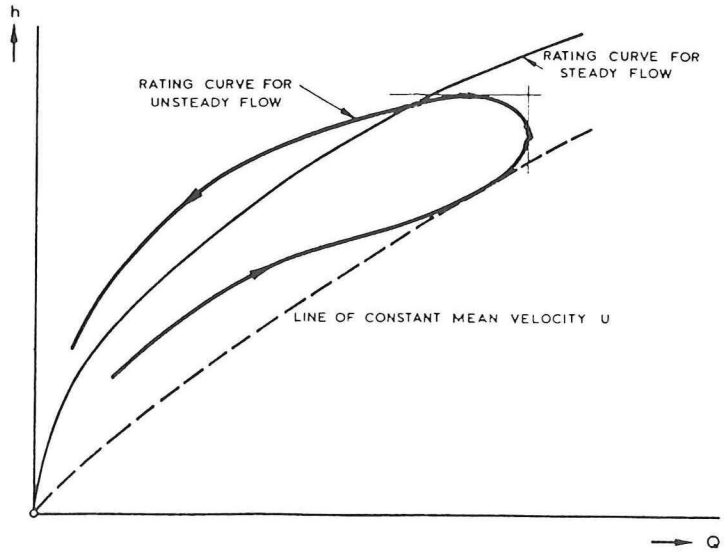

Fig.6 Hysteresis effect

3.4 TRANSPORT PROCESSES

3.4.1 Basic equations

For the description of the transport processes we use the mass balances of the dissolved matter in the main stream and in the stagnant zone.

Convection is the longitudinal transport of a dissolved substance, caused by the flow. Meanwhile, mixing takes place in three dimensions, caused by:

- molecular diffusion
- turbulent diffusion
- dispersion

The influence of molecular diffusion is negligible with regard to turbulent diffusion and dispersion, and therefore usually not taken into account.

The mass balance of a control volume of water is given by:

$$\frac{\partial \overline{\phi}}{\partial t} + \frac{\partial f_x}{\partial x} + \frac{\partial f_y}{\partial y} + k\overline{\phi} = 0 \qquad (3.60)$$

The last term accounts for the disintegration of the dissolved substance if the matter is not conservative. In this study it is assumed that the dissolved substance is conservative. f_x and f_y are the time- and depth averaged values of the mass-fluxes in longitudinal and transversal direction, given by

$$f_x = \overline{u}\,\overline{\phi} + \frac{1}{a}\int_0^a (u'\phi')\,dz + \overline{u''\phi''} \qquad (3.61)$$

$$f_y = \overline{v}\,\overline{\phi} + \frac{1}{a}\int_0^a (v'\phi')\,dz + \overline{v''\phi''} \qquad (3.62)$$

with the overbars indicating depth-averaged, before cross-sectionally averaged, values. In these definitions we recognize three transport processes. The first terms on the right hand side are due to convection with the depth-averaged flow velocity. The second terms represent the dispersive part of the transport due to a variation in the time-averaged convection over the depth. The third terms represent the turbulent diffusive transport. In figure 7 these components are depicted: respectively as $\bar{u}$ (time and depth-averaged velocity); u' (time-averaged local deviation of $\bar{u}$); u'' (turbulent fluctuation). The concentration ϕ is assumed to consist of components analogous to the components of the velocity U.

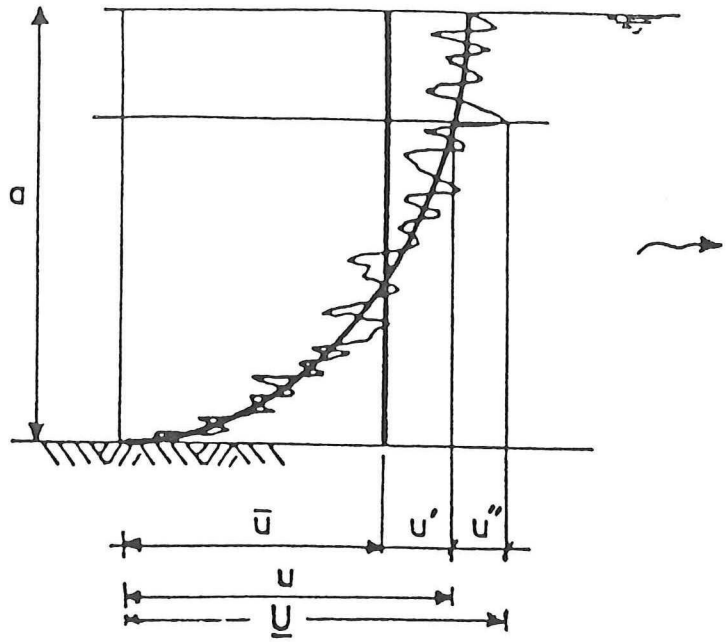

Fig. 7 Components of the velocity in flow direction

It is common to assume that, analogously to molecular diffusion, both the turbulent diffusive transport and the dispersive transport are proportional to the gradient in the concentration of the dissolved matter. This assumption was first made by Taylor (1953,'54), and is only valid on a certain distance from the release-point of the matter, when the depth-averaged concentration curve has reached a symmetric profile.

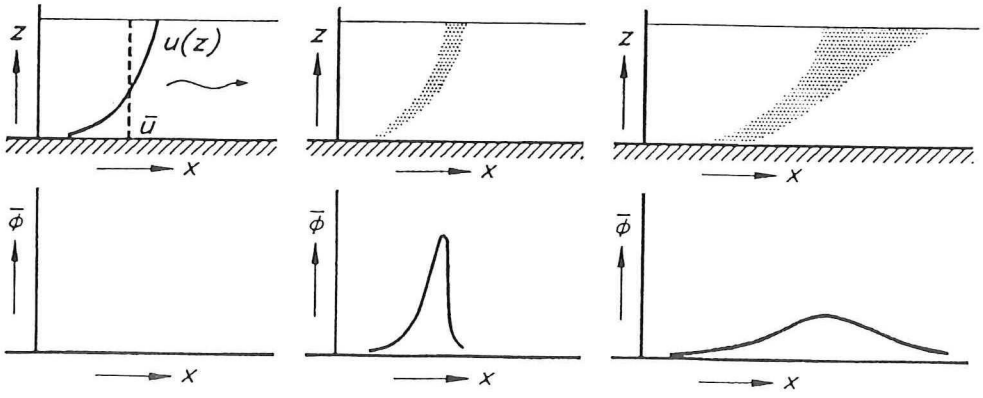

Fig. 8 Dispersion mechanism (after Fischer, 1966)

The depth-averaged flux in x-direction becomes:

$$f_x = \overline{u}\overline{\phi} - K_x \frac{\partial \overline{\phi}}{\partial x} \tag{3.63}$$

Where K_x is the longitudinal dispersion-coefficient. Likewise the depth-averaged flux in y-direction can be written as:

$$f_y = \overline{v}\overline{\phi} - K_y \frac{\partial \overline{\phi}}{\partial y} \tag{3.64}$$

Where K_y is the transversal dispersion-coefficient.

By definition the time- and depth averaged value of v (velocity-component perpendicular to the main flow direction) equals zero, and therefore also the first term of Eq.(3.64), equals zero. Due to cross-sectional variation of the bottom level and riverbends the transversal dispersive flux-term is commonly unequal to zero.

The mass balance, Eq. (3.60), can now be rewritten into :

$$\frac{\partial \overline{\phi}}{\partial t} + \frac{\partial (\overline{\phi}\,\overline{u})}{\partial x} - K_x \frac{\partial^2 \overline{\phi}}{\partial x^2} - K_y \frac{\partial^2 \overline{\phi}}{\partial y^2} = 0 \tag{3.65}$$

When the dissolved matter is not only well mixed over the depth, but also well mixed over the width of the stream near the point of release, a one-dimensional model is satisfying, which means that K_y=0. This assumption is justified in a turbulent mountain river.

$$\frac{\partial \overline{\phi}}{\partial t} + \frac{\partial (\overline{\phi}\,\overline{u})}{\partial x} - K \frac{\partial^2 \overline{\phi}}{\partial x^2} = 0 \tag{3.66}$$

Where K is the one-dimensional longitudinal dispersion coefficient that gives the total dispersion, due to velocity and concentration differences over the entire cross-section. Now the overbars indicate cross-sectionally averaged values of the variables. Again, the *overbars* will be omitted as no unaveraged quantities will be used.

Release of a substance in the flow can be added to the balance by an extra term. In this study this release term will not be added, the tracer release will be taken as an upstream boundary condition in the numerical model.

An analytical solution can be found for the case of an instantaneous release of a pollutant with mass M in a river with steady, uniform flow and a constant cross-sectional area and dispersion coefficient. The mass balance simplifies for this case into:

$$\frac{\partial \phi}{\partial t} + u\frac{\partial \phi}{\partial x} - K\frac{\partial^2 \phi}{\partial x^2} = 0 \qquad (3.67)$$

The analytical solution is given by:

$$\phi(x,t) = \frac{M/A}{2\sqrt{\pi Kt}} \exp\left(\frac{-(x-ut)^2}{4Kt}\right) \qquad (3.68)$$

3.4.2 Integration over the cross-section

To achieve a one-dimensional model in the same dependent variables as the flow-model (cross-sectional area A and discharge Q) the resulting continuity equation (3.65) has to be integrated over the cross-section. While cross-sectionally averaged values are used, a correction coefficient is again introduced in the equation.

$$\frac{\partial \phi aB}{\partial t} + \frac{\partial \phi \alpha_u uaB}{\partial x} - \frac{\partial aBK\frac{\partial \phi}{\partial x}}{\partial x} = 0 \qquad (3.69)$$

Because the effect of a non-uniform geometry is also described by the presence of stagnant zones, an extra term describing the mass flux between the main stream and the stagnant zones has to be added:

$$f_\phi a \Big|_{y=y_r}^{y=y_l} = (\phi - \phi_s) f E u_{ms} a \qquad (3.70)$$

Where:

E	= entrainment coefficient between main stream and stagnant zone	[-]
f_ϕ	= mass flux between main stream and stagnant zones	[kg/m^{3}s]

Using equation (2.14) this yields for the continuity equation:

$$\frac{\partial \phi aB}{\partial t} + \frac{\partial \phi \alpha_u uaB}{\partial x} - \frac{\partial aBK\frac{\partial \phi}{\partial x}}{\partial x} + (\phi - \phi_s) f E \frac{\beta_u}{\alpha_u} ua = 0 \qquad (3.71)$$

Fischer (1979) suggested the following expression for the longitudinal dispersion coefficient:

$$K = 0.0066\frac{u^2B^2}{K_y} = 0.011\frac{u^2B^2}{au_*} \tag{3.72}$$

For a river with a stagnant zone this expression can be rewritten into

$$K = \mu\frac{u_{ms}^2B_{ms}^2}{au_*} = \mu\frac{C}{\sqrt{g_z}}\frac{u_{ms}B_{ms}^2}{a} \tag{3.73}$$

when the friction velocity is defined as

$$u_* = \frac{\sqrt{g_z}}{C}u_{ms} \tag{3.74}$$

Using the definitions for u_{ms}, β_s, A, Q, σ_u (respectively Eqs. (2.14), (2.15), (3.25), (3.26), (3.29)), the third term of Eq. (3.71) can be rewritten into:

$$\begin{aligned}\frac{\partial aBK\frac{\partial\phi}{\partial x}}{\partial x} &= \frac{\partial}{\partial x}\left[aB\left(\mu\frac{C}{\sqrt{g_z}}\frac{u_{ms}B_{ms}^2}{a}\right)\frac{\partial\phi}{\partial x}\right] = \\ = \frac{\mu C}{\sqrt{g_z}}\frac{\beta_u}{\alpha_u}(1-\beta_s)^2\frac{\partial}{\partial x}\left(B^3u\frac{\partial\phi}{\partial x}\right) &= \frac{\mu C}{\sigma_u\sqrt{g_z}}\frac{\partial}{\partial x}\left(\frac{QB^3}{A}\frac{\partial\phi}{\partial x}\right)\end{aligned} \tag{3.75}$$

Substitution of Eq. (3.75) into Eq. (3.71) finally yields :

$$\frac{\partial}{\partial t}(\phi A) + \frac{\partial}{\partial x}(\phi Q) - \frac{\mu C}{\sigma_u\sqrt{g_z}}\frac{\partial}{\partial x}\left(\frac{QB^3}{A}\frac{\partial\phi}{\partial x}\right) + (\phi - \phi_s)fE\sigma_u\frac{Q}{B} = 0 \tag{3.76}$$

Notice that the first two terms can be simplified by satisfying the continuity equation. For the sake of the discretization the continuity equation is slightly rewritten:

$$\begin{aligned}A\frac{\partial\phi}{\partial t} + \left[Q - \left(\frac{\mu C}{\sigma_u\sqrt{g_z}}\right)\frac{\partial}{\partial x}\left(\frac{QB^3}{A}\right)\right]\frac{\partial\phi}{\partial x} + \\ - \left(\frac{\mu C}{\sigma_u\sqrt{g_z}}\right)\left(\frac{QB^3}{A}\right)\frac{\partial^2\phi}{\partial x^2} + (\phi - \phi_s)fE\sigma_u\frac{Q}{B} = 0\end{aligned} \tag{3.77}$$

We can also formulate an equation that uses the mass balance of the dissolved matter in the stagnant zones. Integrated over the cross-sectional area we find:

$$\frac{\partial \phi_s \beta_s f a B}{\partial t} - (\phi - \phi_s) f E \frac{\beta_u}{\alpha_u} u a = 0 \qquad (3.78)$$

Rewriting (3.78) in terms of the dependent variables Q and A:

$$\left(1 - \frac{1}{\sigma_u}\right) f \frac{\partial}{\partial t}(\phi_s A) - (\phi - \phi_s) f E \sigma_u \frac{Q}{B} = 0 \qquad (3.79)$$

- *The use of correction coefficients in the transport model*

The one-dimensional longitudinal dispersion coefficient K represents the total dispersion due to velocity and concentration differences over the entire cross-section. In stead of adding the dispersive term to the equation, it is possible to correct the transport of substance due to non-uniformity of the profiles by introduction of a correction coefficient β_ϕ (analogously to β_u used in the flow model).

This coefficient is introduced when the mass balance is integrated over the cross-sectional area and cross-sectionally averaged values are used (3.69):

$$\frac{\partial}{\partial x}\left(\bar{\phi}\,\alpha_u \bar{u}\bar{a}B - \bar{a}BK\frac{\partial \bar{\phi}}{\partial x}\right) = \frac{\partial}{\partial x}\int_{y_l}^{y_r}\int_{0}^{a}(\phi u)\,dz\,dy = \frac{\partial}{\partial x}\left(\beta_\phi \bar{\phi}\,\bar{u}\bar{a}B\right) \qquad (3.80)$$

The definitions of β_ϕ is analogous to the definitions given before. A better understanding in which way this coefficient corrects the non-uniformity can again be gained by assuming hypothetical distortions of the time-averaged values from the time and cross-sectionally averaged values. Additionally to the definitions of ϵ_a and ϵ_u is defined:

$$\phi(y,z) = \bar{\phi} + \epsilon_\phi(y,z) \Rightarrow \overline{\phi(y,z)} = \bar{\phi} \;;\; \overline{\epsilon_\phi(y,z)} \equiv 0 \qquad (3.81)$$

This yields following expression for β_ϕ:

$$\beta_\phi = \frac{\int_{y_l}^{y_r}\int_{0}^{a} u(y,z)\,\phi(y,z)\,dz\,dy}{\bar{\phi}\bar{u}\bar{a}B} = 1 + \frac{\overline{\epsilon_a \epsilon_u}}{\bar{a}\bar{u}} + \frac{\overline{\epsilon_a \epsilon_\phi}}{\bar{a}\bar{\phi}} + \frac{\overline{\epsilon_u \epsilon_\phi}}{\bar{u}\bar{\phi}} + \frac{\overline{\epsilon_a \epsilon_u \epsilon_\phi}}{\bar{a}\bar{u}\bar{\phi}} \qquad (3.82)$$

The dispersion coefficient can now be expressed in terms of the deviations ϵ:

$$-K\frac{\partial\overline{\phi}}{\partial x} = \left(\frac{\overline{\epsilon_a\epsilon_\phi}}{\overline{a}\,\overline{\phi}} + \frac{\overline{\epsilon_u\epsilon_\phi}}{\overline{u}\,\overline{\phi}} + \frac{\overline{\epsilon_a\epsilon_u\epsilon_\phi}}{\overline{a}\,\overline{u}\,\overline{\phi}}\right)\overline{u}\,\overline{\phi} \tag{3.83}$$

It can be noticed that, in case of uniform distribution of the concentration over the cross-section ($\epsilon_\phi = 0$), $\beta_\phi = \alpha_u$ (3.82) and the dispersive transport equals zero (3.83).

3.5 FLOW AND TRANSPORT SIMULATING MODEL

Eventually flow and transport are described by following equations. In the next chapter these equations are incorporated in numerical schemes.

$$\frac{\partial A}{\partial t} + \frac{\partial Q}{\partial x} = 0 \tag{3.84}$$

$$\frac{\partial Q}{\partial t} + \sigma_u\frac{\partial}{\partial x}\left(\frac{Q^2}{A}\right) + g_z\beta_a A\frac{\partial}{\partial x}\left(\frac{A}{B}\right) = g_x A - \frac{g_z}{C^2}\sigma_u\frac{Q^2}{A^2}B - fE\sigma_u^2\frac{Q^2}{AB} \tag{3.85}$$

$$A\frac{\partial\phi}{\partial t} + \left[Q - \left(\frac{\mu C}{\sigma_u\sqrt{g_z}}\right)\frac{\partial}{\partial x}\left(\frac{QB^3}{A}\right)\right]\frac{\partial\phi}{\partial x} + -\left(\frac{\mu C}{\sigma_u\sqrt{g_z}}\right)\left(\frac{QB^3}{A}\right)\frac{\partial^2\phi}{\partial x^2} + (\phi - \phi_s)fE\sigma_u\frac{Q}{B} = 0 \tag{3.86}$$

$$\left(1 - \frac{1}{\sigma_u}\right)f\frac{\partial}{\partial t}(\phi_s A) - (\phi - \phi_s)fE\sigma_u\frac{Q}{B} = 0 \tag{3.87}$$

In the one-dimensional model following variables, parameters and coefficients are defined:

4 variables: $Q(x,t)$, $A(x,t)$, $\phi(x,t)$, $\phi_s(x,t)$
4 equations (3.84) through (3.87) make the system determined.

parameters:	B_{up}, B_{down}, i_b, a	4
coefficients:	C, fE, f, μ, σ_u, β_a	6
		10 unknowns

While the parameter E only appears in the equations together with the parameter f, it is obvious to identify a parameter fE, defined as $f \cdot E$, in stead of E.

Identification of values for the ten unknown characterizes the irregular geometry of a particular river section of a mountain stream. It has to be reminded that the main objective is the determination of the geometry, the results of which can be applied in simplification of a particular river section. This means that the accuracy of the identified values for B_{up}, B_{down}, i_b, a and C determines the applicability of the identification system, where a is the downstream depth under steady flow conditions and i_b is the average bottom slope.

Additionally values will be identified for β_a, σ_u, μ, fE and f. While the identified value of β_a merely gives an indication of the non-uniformity of the depth over the width of the stream (Appendix A), the value of σ_u is more important. This value, as explained before, represents the coupling between the use of correction coefficients and the stagnant zone concept Eq. (3.29). This means that the identified value of σ_u corrects the flow processes for the presence of dead zones and for the effects of non-uniform distribution of the flow-velocity in main stream direction over the cross-sectional area. Moreover, the possibility exists to rewrite the value of this coefficient into a value of the stagnant zone coefficient β_s, which illustrates the possibility to express corrections for the non-uniformity of the profiles in a geometrical coefficient.

The identified value of μ can be rewritten into an over-all dispersion coefficient K (Eq. (3.72)) that can be applied in a transport simulating model. The identification of values for the coefficients f and fE is the least important. The value of f indicates the fraction of dead zones on the length of the river reach L. The parameter fE that appears in the momentum equation can be understood as an over-all entrainment coefficient with respect to the exchange of momentum and dissolved matter between main stream and stagnant zone. This value too can be used in a transport simulating model.

4 Numerical approach

4.1 NUMERICAL ASPECTS

4.1.1 General

Increased computational capacity together with progress made with respect to numerical analysis has meant that in the recent years more river problems have been tackled using numerical models. To achieve satisfactorily results, a good mathematical description of the physical processes is an absolute prerequisite.

The mathematical description of the flow and transport processes is derived in chapter 3. In this chapter the resulting system of equations (3.84) to (3.87) will be incorporated in numerical schemes. These discretisized equations form the basis of a numerical model capable of describing unsteady flow and transport processes.

The choice of the numerical schemes has to be carried out with great care. Criteria like accuracy and stability are very important. First some characteristics of discretization are treated and a choice will be made for the numerical schemes to be used in this study.

4.1.2 Implicit and explicit schemes

Different methods exist for the transformation of a differential equation into a numerical algorithm. Numerical schemes can be roughly divided in explicit and implicit schemes. An initial value problem is considered:

$$\frac{\partial y}{\partial t} = f(y,t) \tag{4.1}$$

with

$$y(t_0) = y_0 \tag{4.2}$$

In these equations f is a general function, t_0 and y_0 are constants. Note that fore a numerical solution equation (4.2) is a necessary condition. Numerical methods can only deal with problems with unique solutions, unlike analytical methods where a general solution can be presented.

- *Explicit methods*

The derivative (4.1) is estimated by the difference form:

$$\frac{\partial y}{\partial t} \approx \frac{y_n - y_{n-1}}{\Delta t} = f(y_{n-1}, t_{n-1}) \tag{4.3}$$

This means that the solution at each time step is calculated straight forward, because for the evaluation of the function f only known y-values are used.

- *Implicit methods*

If for the evaluation of the function f values of y at the new time step (unknown values) are used, an implicit method results. In this case the calculation of y_0 is no longer straight forward but an algebraic expression needs to be solved. An example of such a method is:

$$\frac{\partial y}{\partial t} \approx \frac{y_n - y_{n-1}}{\Delta t} = \theta f(y_n, t_n) + (1-\theta) f(y_{n-1}, t_{n-1}) \tag{4.4}$$

The parameter θ is a weighing factor, $0 \leq \theta \leq 1$. If $\theta > 0.5$ the weight is mainly put on the new time level, n. $\theta < 0.5$ puts the weigh mainly on the old time level n-1. The case that $\theta = 0$ results in an explicit method.

Although, for the general case, the implicit method is more difficult to handle and requires more computational efforts, it has advantages concerning the stability of the computation.

4.1.3 Stability

If some error is introduced during the numerical computation, e.g. due to the round off error of the computer, this error will grow with the amplification factor ρ. Demanding that this error is kept limited yields the condition for stability:

$$|\rho| \leq 1 \tag{4.5}$$

- *Explicit methods*

The Courant-Friedrichs-Lewy stability analysis shows that in case of explicit methods the Courant number is important:

$$\sigma = \frac{u \Delta t}{\Delta x} \leq 1 \tag{4.6}$$

When this condition is satisfied, the value of a variable at a new time level can be interpolated between known values on the old time level. In the case that $\sigma > 1$, the point on the new time level is outside the numerical influence area which leads to instability.

- *Implicit methods*

For implicit methods it can be shown that the stability condition is fulfilled if $0.5 < \theta < 1$. This means that no restriction is put on the time step, which is an important advantage of implicit methods. This is especially interesting for systems of differential equations with very different relaxation times (the problem of stiffness). The behaviour of such a system is determined by large relaxation times, but when an explicit method is used the smallest time scale determines the time-step restriction due to stability conditions.

4.1.4 Staggered or unstaggered grid

In the flow model two system variables are to be integrated: Q and A. Usually a staggered grid is used for the numerical integration. This means that the grid points are divided into Q points and A points. In many cases a staggered grid is very efficient because the continuity equation contains a time differential in A and a space differential in Q. The equation of motion contains a time differential in Q and a space differential in A. In a staggered grid in space the unknown variables on the new time level can be calculated in every grid point, by connecting the integration molecules.

- *Staggered grid*

An example of an implicit scheme with a staggering grid is the Crank-Nicholson method. The grid should be chosen such that the correct type of points are on the boundaries, where conditions are given. In figure 9 the staggered grid is demonstrated for the Crank-Nicholson molecules.

- *Unstaggered grid*

In this study a staggered grid can not be used, in the first place because the equations describing the transport processes would not fit in a staggered grid. Another problem is that the momentum equation defined by (3.85) needs Q and A values in every grid point. An alternative implicit scheme is the Preissmann scheme, or four-point method. The lay-out of the grid is depicted in figure 10.

The Preissmann method has the advantage that the grid size can be changed easily from one region to another. Moreover, modification of the scheme at the boundaries, where only two grid points are available, is not necessary.

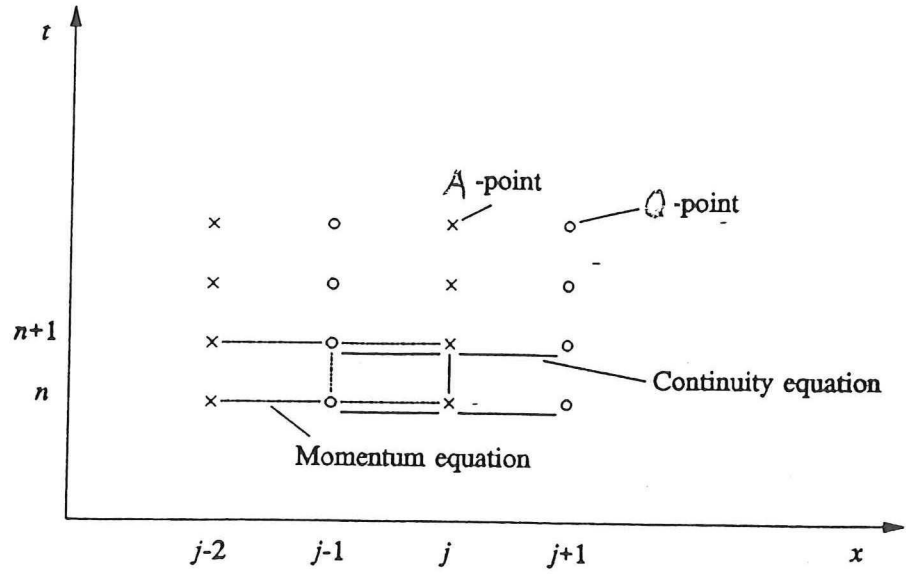

Fig.9 Space-staggered grid for the Crank-Nicholson method

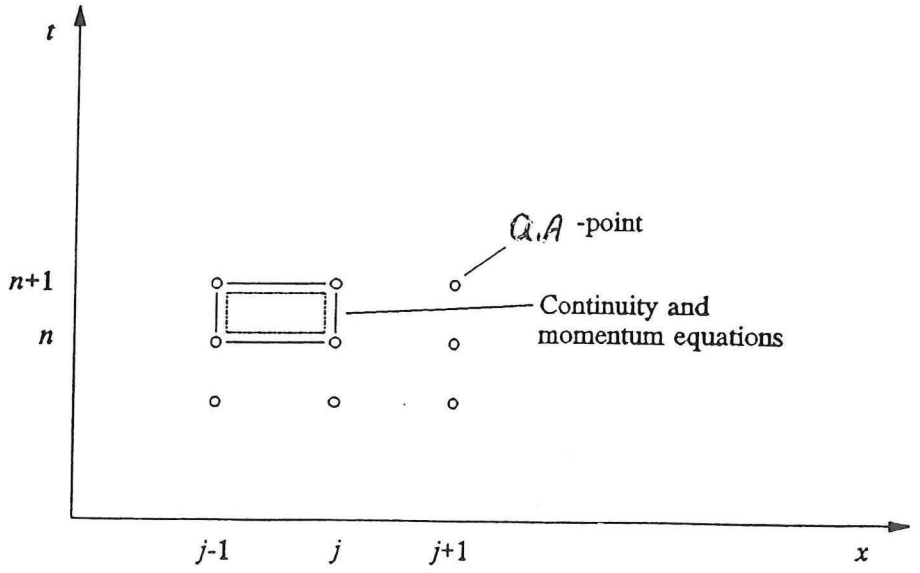

Fig.10 Grid for the Preissmann method

4.1.5 Choice of the numerical schemes

The use of implicit schemes is chosen. These methods are unconditionally stable for $0.5 < \theta < 1$. This means that no restriction is put on the time step, which is especially interesting for systems of differential equations.

Because an unstaggered grid has to be used for discretization of the flow-equations the Preissmann scheme is chosen. The second order derivative in the dispersive term of the continuity equation of the dissolved matter needs at least three spatial grid points. Therefore we use the Crank-Nicholson scheme for discretization of the transport equations. For the case without friction, following expressions can be found for the amplification factors for the two numerical schemes applied in this study:

Preissmann:
$$\rho = \frac{1 \pm 2(1-\theta)\sigma i \tan\xi/2}{1 \pm 2\theta\sigma i \tan\xi/2} \qquad (4.07)$$

Crank-Nicholson:
$$\rho = \frac{1 \pm (1-\theta)\sigma i \sin\xi}{1 \pm \theta\sigma i \sin\xi} \qquad (4.08)$$

The unknown variables are defined below. Given these amplification factors, some parameters can be defined that indicate the accuracy of the numerical approach.

4.1.6 Accuracy

Accuracy of numerical models can be analysed by investigating properties of a propagating wave, such as numerical wave celerity and numerical wave damping. These properties can be expressed in the complex amplification factor ρ of a numerical scheme.

During one time step the numerical solution is multiplied by the amplification factor. This means that the amplitude of the wave is multiplied by $|\rho|$ and that a phase shift by $\arg(\rho)$ occurs. In the transport prediction the difference between the concentration and its equilibrium value is multiplied by $|\rho|$.

Some parameters can be defined that characterize the accuracy of the flow- and transport model.

- *Flow model*

Discretization of the flow model is based on the Preissmann scheme. The complex amplification factor ρ is defined by (4.07). The flood wave parameters in the expression of ρ are defined by:

flood wave celerity	$= c$	$= (\partial Q/\partial h)/B$	[m/s]
flood wave period	$= T$		[s]
length of flood wave	$= L$	$= cT$	[m]
Courant number	$= \sigma$	$= c\Delta t/\Delta x$	[-]
wave number	$= k$	$= 2\pi/L$	[m^{-1}]
relative grid size	$= \xi$	$= k\Delta x$	[-]

The numerical flood wave damping is given by the damping factor d_n.

$$d_n = |\rho|^n \tag{4.9}$$

in which n is the number of time steps. The error in wave propagation speed is represented by c_r. This is the ratio of the of the numerical and analytical wave celerity.

$$c_r = -\frac{\arg(\rho)}{2\pi\,\Delta t/T} \tag{4.10}$$

For accuracy reasons the numerical flood wave damping and the numerical flood wave celerity should not be too deviating from the analytical (true) values. In an ideal model both d_n and c_r tend to unity.

- *Transport model*

Now a propagating concentration cloud is considered. Discretization of the transport equations is based on the Crank-Nicholson scheme. The amplification factor is now defined by (4.08) where some of the parameters are re-defined:

flow velocity	$= u$		[m/s]
length of the cloud	$= L$		[m]
flood wave period	$= T$	$= L/u$	[s]
Courant number	$= \sigma$	$= u\Delta t/\Delta x$	[-]
wave number	$= k$	$= 2\pi/L$	[m^{-1}]
relative grid size	$= \xi$	$= k\Delta x$	[-]

Even if the diffusion-/dispersion coefficient (K, Eq. (3.72)) equals zero, diffusion in the model may occur due to numerical effects. A parameter that indicates these numerical effects on the transport of substance is the numerical diffusion coefficient, given by:

$$K_{num} = \left(\theta - \frac{1}{2}\right) u^2 \Delta t \tag{4.11}$$

This value is positive if $\theta \geq 0.5$.

4.1.7 Wiggles

In some cases the numerical solution of the convection-diffusion equations shows *wiggles*, short waves with wave length $2\Delta x$. This is a form of inaccuracy but not of instability because the waves do not grow in time. Wiggles are usually caused by large concentration gradients and therefore often occur with a sudden change at the boundary (for example a sudden start or stop of a dissolved matter release). These oscillations can be prevented by satisfying the condition:

$$P = \frac{u \Delta x}{K} \leq 2 \tag{4.12}$$

In which P is the Cell-Péclet number. Wiggles do not necessarily occur if $P > 2$. This strongly depends on the boundary conditions. For a continuous release of a dissolvant the concentration gradients will be small, which makes the system more immune to wiggles. In the case of an instantaneous tracer release larger gradients in the concentration curve, and therefore wiggles, are more likely to occur.

4.2 NUMERICAL MODEL

4.2.1 Discretization of the flow equations

Solutions of differential equations are usually continuous functions in the time-space domain. In solving the equations numerically it is attempted to find solutions at a finite number of grid points. This is done by replacing the differential equations by difference equations.

For the discretization of the two equations of the flow model (3.84) and (3.85) the Preissmann scheme was used. For the continuity equation this yields:

$$\frac{1}{2}\left(\frac{A_{j-1}^{n+1} - A_{j-1}^{n}}{\Delta t} + \frac{A_{j}^{n+1} - A_{j}^{n}}{\Delta t}\right) + \theta \frac{Q_{j}^{n+1} - Q_{j-1}^{n+1}}{\Delta x} + (1-\theta) \frac{Q_{j}^{n} - Q_{j-1}^{n}}{\Delta x} = 0 \tag{4.13}$$

In order to simplify the momentum equation the friction and the exchange term (together responsible for the total energy dissipation) are taken together as in Eq. (3.30). Discretization of the equation of motion:

$$\frac{1}{2}\left(\frac{Q_{j-1}^{n+1}-Q_{j-1}^{n}}{\Delta t}+\frac{Q_{j}^{n+1}-Q_{j}^{n}}{\Delta t}\right)+$$

$$+\sigma_u\theta\frac{\left[\frac{Q_j^n}{A_j^n}\right]Q_j^{n+1}-\left[\frac{Q_{j-1}^n}{A_{j-1}^n}\right]Q_{j-1}^{n+1}}{\Delta x}+\sigma_u(1-\theta)\frac{\left[\frac{Q_j^n}{A_j^n}\right]Q_j^{n}-\left[\frac{Q_{j-1}^n}{A_{j-1}^n}\right]Q_{j-1}^{n}}{\Delta x}+$$

$$+g_z\beta_a\left(\frac{A_{j-1}^n+A_j^n}{2}\right)\left(\theta\frac{\left[\frac{A_j^{n+1}}{B_j}\right]-\left[\frac{A_{j-1}^{n+1}}{B_{j-1}}\right]}{\Delta x}+(1-\theta)\frac{\left[\frac{A_j^{n}}{B_j}\right]-\left[\frac{A_{j-1}^{n}}{B_{j-1}}\right]}{\Delta x}\right)+$$

$$-g_x\frac{1}{2}\left(\theta\left[A_{j-1}^{n+1}+A_j^{n+1}\right]+(1-\theta)\left[A_{j-1}^{n}+A_j^{n}\right]\right)+$$

$$+\frac{1}{2}\left[\frac{g_z}{C^2}\sigma_u B_{j-1}+fE\sigma_u^2\left(\frac{A_{j-1}^n}{B_{j-1}}\right)\right]\left[\frac{Q}{A^2}\right]_{j-1}^{n}\left(\theta Q_{j-1}^{n+1}+(1-\theta)Q_{j-1}^{n}\right)+$$

$$+\frac{1}{2}\left[\frac{g_z}{C^2}\sigma_u B_j+fE\sigma_u^2\left(\frac{A_j^n}{B_j}\right)\right]\left[\frac{Q}{A^2}\right]_{j}^{n}\left(\theta Q_{j}^{n+1}+(1-\theta)Q_{j}^{n}\right)=0 \qquad (4.14)$$

4.2.2 Boundary conditions of the flow model

Computation of the system variables on a new time step means solving the system of equations. If the spatial grid has m points and two boundary conditions are given, then there are $2*m$-2 unknown values (for Q and A) at the new time level. We have a continuity and a momentum equation for every cell. This means there are $2*(m$-1) equations available, equalling the number of unknown. This makes the system determined and can be solved using the Thomas algorithm.

In the flow model subcritical flow is assumed. This means that an upstream and a downstream boundary condition are necessary (subsection 3.3.3). The downstream condition can be a steady discharge relationship (Q-h curve), for example the simple wave formula

$$\frac{\partial A}{\partial t} + c\frac{\partial A}{\partial x} = Bci_b \tag{4.15}$$

in which c is the celerity of the flood wave. However, if the discharge Q and the water level h do not have a unique relationship during a flood wave (hysteresis-effect), the Jones formula has to be applied Eq. (3.59):

$$Q = Q_s\sqrt{1 + \frac{1}{i_b c}\frac{\partial h}{\partial t}} \tag{4.16}$$

In which Q_s is the steady discharge. Discretization of this equation can be based on the Preissmann scheme. The upstream boundary condition is the measured unsteady river discharge.

4.2.3 Discretization of the transport equations

For the discretization of the continuity equations of the dissolved matter in the mainstream and in the stagnant zones the Crank-Nicholson scheme was used.

Continuity equation (3.86) of the dissolved matter in the main stream:

$$A_j^{\,n}\frac{\phi_j^{n+1} - \phi_j^n}{\Delta t} +$$

$$+ k_{u_j}^{\,n+1}\theta\frac{\phi_{j+1}^{n+1} - \phi_{j-1}^{n+1}}{2\Delta x} + k_{u_j}^{\,n}(1-\theta)\frac{\phi_{j+1}^{n} - \phi_{j-1}^{n}}{2\Delta x} +$$

$$- K_{u_j}^{\,n+1}\theta\frac{\phi_{j+1}^{n+1} - 2\phi_j^{n+1} + \phi_{j-1}^{n+1}}{\Delta x^2} - K_{u_j}^{\,n}(1-\theta)\frac{\phi_{j+1}^{n} - 2\phi_j^{n} + \phi_{j-1}^{n}}{\Delta x^2} +$$

$$+ \theta\left(\phi_j^{n+1} - \phi_{s_j}^{\,n+1}\right)fE\sigma_u\left[\frac{Q}{B}\right]_j^{n+1} + (1-\theta)\left(\phi_j^{n} - \phi_{s_j}^{\,n}\right)fE\sigma_u\left[\frac{Q}{B}\right]_j^{n} = 0 \tag{4.17}$$

Where:

$$k_{u_j}^{\ n} = Q_j^n - \left(\frac{\mu C}{\sigma_u \sqrt{g_z}}\right)\left[\frac{\left(\frac{QB^3}{A}\right)_{j+1}^{n} - \left(\frac{QB^3}{A}\right)_{j-1}^{n}}{2\Delta x}\right] \tag{4.18}$$

$$K_{u_j}^{\ n} = \left(\frac{\mu C}{\sigma_u \sqrt{g_z}}\right)\left[\frac{QB^3}{A}\right]_j^n \tag{4.19}$$

Continuity equation (3.87) of the stagnant zones:

$$\left(1-\frac{1}{\sigma_u}\right) f \frac{\phi_{s_j}^{\ n+1} A_j^{n+1} - \phi_{s_j}^{\ n} A_j^n}{\Delta t} +$$

$$-\theta\left(\phi_j^{n+1} - \phi_{s_j}^{\ n+1}\right) f E \sigma_u \left[\frac{Q}{B}\right]_j^{n+1} - (1-\theta)\left(\phi_j^n - \phi_{s_j}^{\ n}\right) f E \sigma_u \left[\frac{Q}{B}\right]_j^n = 0 \tag{4.20}$$

4.2.4 Boundary conditions of the transport model

At the upstream grid point the concentration is a boundary condition, determined by the tracer release:

$$\phi_1^{n+1} = \phi_0 + \frac{M}{Q_1^{n+1}} \tag{4.21}$$

A constant release (M [kg/s]) of the trace is assumed in a river with a natural background concentration ϕ_0. Because of the second order derivative in the dispersive term, a numerical scheme is used (Crank-Nicholson) that requires at least three spacial grid points. At the downstream boundary only two grid points are available, which means that a second order derivative cannot be incorporated in this last cell. In this boundary, gridpoint $j=m$, the equation simplifies and can be discretisized if the Neumann condition is used

$$\frac{\partial \phi}{\partial x}\Big|_{j=m} = \frac{\phi_m - \phi_{m-1}}{\Delta x} = \text{const.} \tag{4.22}$$

5 The parameter identification system

5.1 DESCRIPTION OF THE MODELS

5.1.1 General

In chapter 3 equations were derived describing the flow and transport processes in an irregular mountain stream under flood wave conditions. In chapter 4 the flow and transport description was approached numerically. The discretisized equations, together with initial and boundary condition, enable numerical computation of the system variables Q and A, on discrete intervals of a certain river section and time interval.

The numerical approach of chapter 4 is the basis of two numerical models: *Identify* and *Simulate*. The models are written in the programming language MATLAB, which is a powerful tool in algebraic computation.

Because a numerical model can only be run if values for the system-parameters are given, first order estimates are necessary. Based on wave propagation phenomena, discussed in section 3.3, expressions for the system-parameters are given in section 5.2.

First in subsection 5.1.2 the two numerical models are described. Both models are based on the same flow and transport description and use the same numerical approach. Both contain two elementary modula: A flow and a transport module. In subsection 5.1.3 the parameter identification system is described, developed to characterize a non-uniform geometry, the purpose of this study.

5.1.2 Flow and transport simulating models

- *Identify*

An upstream measured water level is used as a boundary condition in the flow model. As a downstream boundary condition the simple wave, or Jones formula can be applied. This has the advantage that an observation of the downstream water level is produced. The transport module produces an observation of the downstream concentration curve. The length of the river section and the amount of tracer release have to be given. First order estimates of the parameter-values, necessary to run the model, are based on the expressions given in section 5.2.

Both produced downstream observations (water level and concentration) can be compared with measured curves. The alikeness of the observed (produced by *Identify*) and measured curves gives an indication of the quality of the parameter-values. The model is called *Identify* because this is the first step in the identification of values for the system-parameters describing the irregular river geometry. Resulting values of this first identification step can be updated to find a best set of parameter-values. This is a parameter identification problem, described in subsection 5.1.3.

An additional result of this model is a first indication of the upstream discharge curve. If the values of the system variables are updated, also a better approach of the upstream discharge will be obtained.

- *Simulate*

To run the model *Identify*, measurements of water levels and of a downstream concentration curve are needed. These measurements can, of course, be taken from a natural river. But to test the model it is convenient to be able to produce measurements numerically: Synthetic measurements. This model provides in this.

The model uses a known upstream discharge curve as a boundary condition in the flow module. Again the Jones formula is used as a downstream condition. This makes the downstream water level a result of the computation.

Again values of the system parameters are necessary to run the model. Now the user of the model has the possibility to define the upstream unsteady discharge and the river geometry, as well as values for the hydraulic and correction coefficients. In this way it is possible to *simulate* flow and transport in a fictive river under flood wave conditions. Results of this model are synthetic measurements of the upstream and downstream water level and downstream concentration curve, continously in time for a period longer than the wave period. These measurements can be used to test the model *Identify* and the parameter identification system.

5.1.3 The parameter identification system

- *General*

The purpose is to develop a method that identifies values for parameters describing a non-uniform river geometry, for example that of a mountain river. The determination of the parameter-values of a system of equations is an identification problem. The identification is merely based on following information:

Continuous measurements of:

- $h(0,t)$: water level at x=0 [m]
- $h(L,t)$: water level at x=L [m]
- $\phi(L,t)$: concentration at x=L [kg/m^3]

Additional data:

- L : length of river section [m]
- ϕ_0 : background concentration for x<0 [kg/m^3]
- M : quantity of tracer release [kg/s]

Based on this data first order estimates of the parameter values are found and an identification of the best set of parameter-values is carried out. The identified set of parameter-values characterizes the irregular geometry of a particular river section. For a general consideration following variables are defined:

Θ = vector containing the parameters to be identified
p = number of elements in Θ
$f(\Theta)$ = vector containing the observations produced by *Identify*
Y = vector containing the measurements
n = number of elements in Y and $f(\Theta)$
$J(\Theta)$ = $\| Y\text{-}f(\Theta) \|^2$ = cost function to be minimized

The observations are a function of the parameter-values and therefore the observation vector $f(\Theta)$ is a function of the parameter vector Θ. The identification is based on finding values for the parameters of the vector Θ that yield observations $f(\Theta)$ that coincide with the measurements Y. In other words: The alikeness of the vectors $f(\Theta)$ and Y indicates the quality of the parameter-values in Θ. This is expressed by the cost function $J(\Theta)$. If this function is minimized, the observation-vector $f(\Theta)$ converges to the measurement-vector Y. The values of the parameter-vector Θ for which the cost function is minimized, characterize the geometry of a particular river section.

In this study the variables are defined by:

$$\Theta = [\ B_{up}\ B_{down}\ i_b\ a\ \mu\ \beta_a\ \sigma_u\ C\ f\ fE\ ]^T \quad (5.1)$$

$$p = 10 \quad (5.2)$$

$$f(\Theta) = [\ h(L,0) \ldots h(L,T)\ \phi(L,0) \ldots \phi(L,T)\ ]^T\ ; \quad \text{observations} \quad (5.3)$$

$$Y = [\ h(L,0) \ldots h(L,T)\ \phi(L,0) \ldots \phi(L,T)\ ]^T\ ; \quad \text{measurements} \quad (5.4)$$

$$n = 2(T/\Delta t + 1) = 2 \text{ x number of time steps} \quad (5.5)$$

$$J(\Theta) = \Sigma[Y_i - f(\Theta)_i]^2\ ; \quad i=1,..,n \quad (5.6)$$

The relevance of identification of the different parameters is explained in section 3.5. Where the observations are generated by *Identify*. The measurements are taken from a natural river or can be synthetically generated, for example with the model *Simulate*.

Usually parameter identification systems investigate the influence of each parameter on each observation (i.e. the influence of each Θ-element on each $f(\Theta)$-element). The heart of such a procedure is the derivative $\partial f(\Theta)/\partial\Theta$. This is a Jacobian matrix, which determination is a significant time and memory consuming operation. For one iteration, p function evaluations are required. In the identification problem of this study, one function evaluation means a complete time loop of the flood wave reconstruction.

- *DUD (Doesn't Use Derivatives)*

An attractive alternative for parameter identification is the procedure DUD (Doesn't Use Derivatives, Ralston and Jennrich 1978). DUD is a derivative free algorithm, that gives a parameter improvement iteration for each function evaluation (instead of p evaluations).

DUD needs $p+1$ function evaluations ($p+1$ vectors $f(\Theta)$ and values $J(\Theta)$), generated using different parameter-vectors Θ (non-singular, stretching a p-dimensional space), before a new Θ (improved parameter-vector) can be created. The $p+1$ parameter-vectors to start with are one parameter vector that contains first order estimates of the parameter-values (based on expressions that will be given in section 5.2), and p vectors that are based on this vector including an arbitrary deviation. The vectors Θ and $f(\Theta)$ must be stored in matrices, such that the requirement is fulfilled that:

$$J(\Theta_1) \geq \ldots \geq J(\Theta_k) \geq \ldots \geq J(\Theta_{p+1}) \tag{5.7}$$

Implying that iteration $p+1$ is the evaluation with the lowest cost function (the best). To enable computation of an improved parameter-vector two more matrices are defined:

$$\Delta\Theta = [\Delta\Theta_1 \ \ldots \ \Delta\Theta_p] \quad ; \quad \Delta\Theta_i = \Theta_i - \Theta_{p+1} \quad ; \quad i = 1 \ldots p \tag{5.8}$$

$$\Delta F = [\Delta F_1 \ \ldots \ \Delta F_p] \quad ; \quad \Delta F_i = f(\Theta_i) - f(\Theta_{p+1}) \quad ; \quad i = 1 \ldots p \tag{5.9}$$

Where:
Θ_i = parameter-vector Θ, defined by Eq. (5.1), underlying the ith iteration.
$f(\Theta_i)$ = observation-vector $f(\Theta)$, defined by Eq. (5.3), resulting from the ith iteration.

Which means that $\Delta\Theta_i$ and $\Delta f(\Theta_i)$ are columns containing respectively p and n elements and that the sizes of the matrices are pxp and nxp. DUD's linear approximation of a new parameter vector is written as a function of α (a vector in the p-dimensional Θ-space):

$$\Theta_{new} = \Theta_{p+1} + \Delta\Theta\,\alpha \tag{5.10}$$

The linear approximation l of f is given by:

$$l(\alpha) = f(\Theta_{p+1}) + \Delta F\,\alpha \tag{5.11}$$

The residue of the linear approximation has to be minimized:

$$J_{l(\alpha)} = \|Y - l(\alpha)\|^2 \tag{5.12}$$

The solution is given by:

$$\alpha = (\Delta F'\Delta F)^{-1}\Delta F'(Y - f(\Theta_{p+1})) \tag{5.13}$$

The algorithm of the identification procedure can be described by:

Executed by *Identify*:
1. Compute the first order parameter vector Θ (expressions section 5.2)
2. Generate $p+1$ Θ-vectors (5.1), non-singular, stretching a p-dimensional space
3. Generate the corresponding observations $f(\Theta)$ Eq. (5.3)
4. Compute their cost functions $J(\Theta)$ by Eq. (5.6)
5. Store the vectors Θ and $f(\Theta)$ in matrices, satisfying Eq. (5.7)
6. Define ΔΘ and ΔF by equations (5.8) and (5.9)

Executed by the DUD parameter identification procedure:
7. Find the vector α from the linear system Eq. (5.13)
8. Compute the new Θ-vector (Θ_{new}) by Eq. (5.10)
9. Execute *Identify*[1], resulting in a function evaluation $f(\Theta_{new})$
10. Compute the cost function J_{new} Eq. (5.6)
11. Renumber the vectors Θ and $f(\Theta)$ according to Eq. (5.7)
    now $p+1$ function evaluations (Θ- and $f(\Theta)$-vectors) are available
12. Erase Θ_1 and $f(\Theta_1)$ (the vectors with the highest cost function)
    now p function evaluations (Θ- and $f(\Theta)$-vectors) are available
13. Compute ΔΘ and ΔF by equations (5.8) and (5.9)
14. Return to step 7, until a specific convergence criterion is satisfied

[1] The flow- and transport-modula of *Identify* generate new observations of a downstream water level and concentration curve.

When the convergence criterion is satisfied, the vector Θ_{p+1} represents the river geometry for which the cost function is minimized. This means that the observations $f(\Theta_{p+1})$ are the best approach of the measurements (Y).

The structure of the parameter identification procedure is depicted in the figure below. The numbers in the figure agree with the steps of the identification procedure.

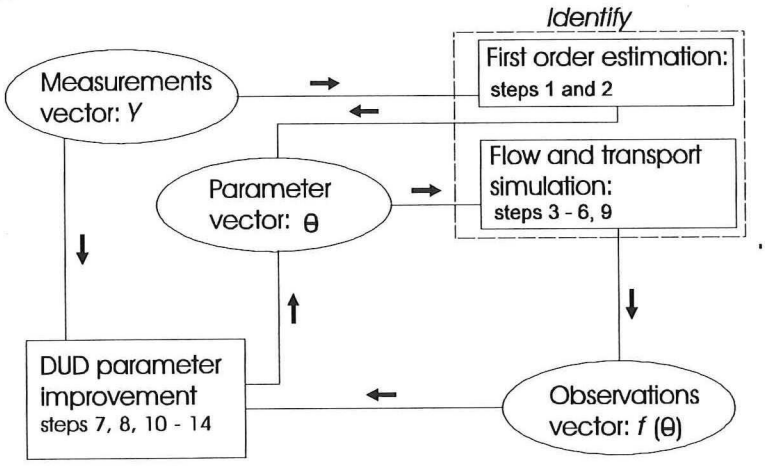

Fig.11 Parameter identification structure

5.2 FIRST ORDER PARAMETER-VALUE ESTIMATION

Based on the relevance of the friction, different approaches of flood wave phenomena were discussed in section 3.3. In order to run a numerical model, values for the system-parameters have to be given. In this section expressions are derived for the system-parameters, based on the same two extreme cases distinguished before: The case of negligible and the case of predominating frictional effects, with respect to inertial effects.

A first estimate of the unsteady river discharge is given by the steady state formula (compare with (2.1)))

$$Q_m(t) = \frac{M}{\phi(L,t) - \phi_0} \tag{5.14}$$

Q_m is considered a 'measured' discharge replacing the measured downstream concentration that contains a phase shift with regard to the unknown $Q(0,t)$. Besides, its shape is distorted by dispersion, unsteady velocities and dead zones.

Reasonable first order approximations can be found in:

$$Q_{\min} = \min(Q_m) \tag{5.15}$$

$$Q_{max} = \max(Q_m) \tag{5.16}$$

$$i_b = \frac{\min(h(0,t)) - \min(h(L,t))}{L} \tag{5.17}$$

$$c = \frac{L}{t[\max(h(L,t))] - t[\max(h(0,t))]} \tag{5.18}$$

$$u = \frac{L}{t[\max(Q_m(t))] - t[\max(h(0,t))]} \tag{5.19}$$

Because, until now, values for the parameters are not yet available, based on trial and error and some common sense, the relevance of the frictional effects has to be estimated.

- *Approach 1: Negligible friction*

In this first order estimation, a value for the water depth in steady flow is derived from the propagation speed of the flood wave which approaches the speed c of small disturbances in the water surface. In case that the variables are uniformly distributed over the width (α_u=1 and β_u=1) and no stagnant zone is present (β_s=0), the defined variable σ_u=1 and c is defined by Eq. (3.43), subsection 3.3.3:

$$c = u + \sqrt{g_z a_0} \quad \Rightarrow \quad a_0 = \frac{(c-u)^2}{g_z} \tag{5.20}$$

This yields:

$$z_{down} = \min(h(L,t)) - a_0 \tag{5.21}$$

- *Approach 2: Predominating friction*

In this approach the water depth is derived from the kinematic approach (subsection 3.3.6). This meas that, in spite of the hysteresis effect, a direct relationship between the discharge and the depth is supposed: the rating curve for steady flow Eq. (3.51). In case of uniformly distributed variables this relation is given by:

$$Q(L,t) = B_{ms} C \sqrt{i_b} \left[h(L,t) - z_{down} \right]^{3/2} \tag{5.22}$$

In other words, change in the depth results in a proportional change in discharge. From this point of view an other expression can be found for the depth downstream. First a variable *ratio* is defined:

$$ratio = \left(\frac{Q_{\max}}{Q_{\min}} \right)^{2/3} \tag{5.23}$$

The value of *ratio* is known from Eqs. (5.15) and (5.16). Substitution of Eq. (5.22) in (5.23) yields an expression for the unknown downstream bed-level:

$$Z_{down} = \frac{\max(h(L,t)) - ratio \cdot \min(h(L,t))}{1 - ratio} \tag{5.24}$$

$$a_0 = \min(h(L,t)) - z_{down} \tag{5.25}$$

Using either one of the approaches to find a first order estimate for the downstream water depth a_0, following expressions yield values for the other parameters.

$$z_{up} = z_{down} + i_b L \tag{5.26}$$

$$B_{up} = \frac{Q_{\min}}{a_0 u} \tag{5.27}$$

$$B_{down} = B_{up} \tag{5.28}$$

Although based on the kinematic approach, a good first order estimate of the friction coefficient can be found in

$$C = \frac{u}{\left[i_b \left(\max(h(L,t)) - z_{down} \right) \right]^{1/2}} \tag{5.29}$$

First order estimates for the other parameters are based on the following assumptions:

$$\mu = 0.011 \tag{5.30}$$

$$\beta_a = 1.00 \tag{5.31}$$

In literature values can be found for the stagnant zone coefficient. For a mountain stream with large boulders, a stagnant zone of 5 %, relative to the total cross sectional area, seems reasonable.

$$\beta_s = 0.05 \quad \Rightarrow \quad \sigma_u = \frac{1}{1-\beta_s} \approx 1.05 \tag{5.32}$$

Analogously to Ω Eq. (3.44) (ratio between frictional and inertial effects) we can define a coefficient which represents the ratio of the maximum values of the exchange term and the local inertia

$$\Xi = \frac{fE\sigma_u^2}{\omega}\frac{u_{\max}}{B} \tag{5.33}$$

This shows the dependency between the stagnant zone parameters β_s (stagnant zone coefficient), f (stagnant zone fraction on the length L), and E (entrainment coefficient). If the effects of momentum exchange are assumed to be in the same order of magnitude as the inertial effects, this relation yields values for these parameters.

For example: A flood wave with a period of 4000 minutes, in a mountain stream with a width B=10 [m] and a mean velocity u=0.15 [m/s] yields:

$$f = 0.10 \tag{5.34}$$

$$fE = 0.0015 \tag{5.35}$$

6 Numerical experiments

6.1 INTRODUCTION

To test the parameter identification system (the model *Identify* integrated with the parameter identification procedure DUD), several cases are carried out. Although the objective is to characterize the unknown river geometry, an additional result will be the reconstruction of the upstream unsteady discharge, unknown so far.

As explained in chapter 5, the upstream measured water level $h(0,t)$ is an upstream boundary condition in the flow module. As a downstream boundary condition $h(L,t)$ can be taken, or the simple wave or Jones formula. Using either one of the formula has the great advantage that a new observation of $h(L,t)$ is generated. This observed downstream water level, together with the observed downstream concentration-curve, are compared with the measurements. The alikeness of the observations, generated by *Identify*, and the measurements indicates how well the original geometry is reconstructed. The result of the identification procedure is a best parameter-vector whose values characterize the geometry of a particular river section.

Before testing the ability of the system to identify a river geometry, verification tests have to be carried out. These tests verify if the flow and transport processes are modelled correctly and if the system is capable of finding a discharge and a geometry that yield observations equal to the measurements. Because the observations produced by the model *Identify* are based on the same mathematical description and on the same numerical schemes as the measurements that are generated by *Simulate*, measurements have to be used in the verification that are generated by other numerical models. In section 6.2 these verification-tests are described.

In section 6.3 test-cases are described that are carried out to identify a river geometry. Values of the identified parameter-vector are compared with values of the original vector underlying the 'true' measurements.

6.2 VERIFICATION OF THE MODEL

6.2.1 General

Two verification-tests are performed. In the first testcase measurements are used that were generated by a flow and transport simulating model with place and time dependent variables written by Meijer (1992). The measurements were used to reconstruct an unsteady discharge. The observed discharge, reconstructed by the identification system, will be compared with the 'true' discharge that was used as a boundary condition.

After that a testcase is carried out that uses measurements that are generated by TRISULA (Delft Hydraulics). This program simulates a dilution test under unsteady flow conditions using unknown numerical schemes and an unknown river geometry. The measurements were used by Meijer to verify his numerical model.

6.2.2 Model performance

- *First verification-test*

The reconstructed unsteady upstream discharge agrees well with the discharge that was used as a boundary condition in the simulation model written by Meijer (Appendix B). This is a first indication that we can have confidence in the identification procedure. An additional result is now the optimized river geometry. But because the 'true' geometry is unknown, it is not possible to compare the results.

- *Second verification-test*

In this case the reconstructed discharge deviates more from the discharge that was used as a boundary condition in TRISULA to simulate measurements, but still we can have confidence in the procedure. Appendix C shows the reconstructed and measured discharge. The reconstructed discharge agrees even better if it is compared with the discharge identified by Meijer (1992).

6.3 CHARACTERIZATION OF THE NON-UNIFORM GEOMETRY

6.3.1 General

Now verification of the model has shown that the parameter-identification system is able to reconstruct satisfactory an unknown unsteady discharge, we can perform tests with the purpose to characterize an unknown geometry. The unsteady discharge will be an additional result.

In the subsections 6.3.2 and 6.3.3 the flow- and transport simulating model *Simulate* (chapter 5), is used to generate measurements. Identification results in best values of the parameter-vector describing the geometry and a reconstructed upstream unsteady discharge. The identified parameter-values are compared with the 'true' parameter-values and the reconstructed discharge is compared with the discharge that is used as a boundary condition in the model *Simulate*.

Subsections 6.3.4 and 6.3.5 describe independent cases to test the robustness of the parameter identification system. The tests are based on measurements generated by the model TRISULA (Delft Hydraulics).

In the subsections 6.3.2 and 6.3.3 first order estimates of the parameter values are found based on the assumption of predominating frictional effects (section 5.2). It turns out that this approach is not useful for the testcase described in subsection 6.3.4. In this case a negligible friction is assumed to gain first order estimates of the parameter values.

6.3.2 Case 1 based on measurements generated by *Simulate*

- *Description*

This case tests the influence of the hydraulic and correction coefficients on the behaviour of the flow and the transport processes. A moderate geometry is defined: a mild bottom slope, uniform width and moderate bed roughness. If a parameter value is identified that agrees well with the value that underlies the measurements, then the influence of this parameter is proportional.

- *Results*

The system succeeds in identification of a geometry and reconstruction of a discharge yielding observations that match the measurements. The reconstructed unsteady discharge matches the measured discharge very well (Appendix D).

In the schedule the resulting parameter-vector is given. The largest deviations occur in the values that are found for the parameters f and fE. It has to be notified that the parameter f only ones occurs independent in a term of the transport equation which explains its limited influence on flow and transport processes. This means that it is difficult to define a fraction of dead zones on the length of a river section. With respect to the use of the identified values in a flow model this parameter has no importance. The difficulty in the identification of fE can be explained by the contribution of the exchange term to the total energy dissipation Eq. (3.30), which is twenty times smaller than the contribution of the friction.

The results show that the correction coefficients σ_u and β_u, as well as the dispersion coefficient μ, have a proportional influence on the hydraulic processes.

6.3.3 Case 2 based on measurements generated by *Simulate*

- *Description*

The geometry defined in this case has a better resemblance with a 'real' mountain stream: steeper bottom slope, larger stagnant zone fraction and bed roughness.

- *Results*

Appendix E shows that the system succeeds in identification of a geometry whereby the produced observations of the downstream water level and concentration and upstream discharge equal the measurements. Nevertheless we can conclude from the schedule that larger deviations occur in the identified geometry from the 'real' geometry than in the first testcase. While the river bottom in this case is even rougher than in the first case, it is obvious that the largest deviations again occur in the identified values for f and fE.

An interesting image is taken up in Appendix F and shows successive iterations in convergence of the DUD-procedure.

6.3.4 Case 1 based on measurements generated by TRISULA

- *Description*

In this case the downstream water level is used as a boundary condition. This means that the generated downstream water level gives no longer an indication of the quality of the reconstructed geometry.

- *Results*

Results of two runs of the identification procedure can be found in Appendix G. The two runs are based on different first order estimates of the parameter-vector. The graphical results show that both observed concentration curves satisfactorily approach the measurement and that the reconstructed flood waves coincide with the unsteady discharge that was used as a boundary condition.

The schedule summarizes the identified parameter-values. It can be noticed that one of the identified geometries coincides very well with the true geometry. The deviation in this identification is expressed in percentages. The other identification, on the other hand, results in a very inaccurate approach, although the quality of the matching reconstructed discharge is satisfying.

The bad representation of the geometry is a result of the first run of the identification system, in which first order estimates are based on expressions that are derived in chapter 5 (by assuming a negligible friction). When comparing of the identified with the true geometry turned out that the results were inaccurate, the second testcase was run. The first order estimates that are used in this second run are based on the true parameter-values including arbitrary deviations of 15 %. The results show that the identification procedure in this case converges towards the true geometry.

The additional parameters f, fE and β_a are not explicitly defined in TRISULA. The 'true' value of f equels one by definition, which indicates an over-all pressence of stagnant zones on the lenght L. The identified value deviates in an extreme way because of the limited influence of this parameter. The identified value for σ_u can be rewritten in a stagnant zone coefficient β_s (Eq. 3.29), which enables comparing. The identified value matches well with the input-value used in TRISULA.

To enable comparing of the dispersion-coefficients, the identified value for μ is rewritten into a coefficient K (Eq. 3.72). The identified values for this coefficient deviate in an extreme way from its input-value. This may be explained by the order of magnitude of the dispersion term with respect to the magnitude of the advection term (Eq. 3.86): the dispersional effects are 5250 times smaller.

Apparently, depending on the first order estimated geometry, the identification procedure is able to converge towards different parameter-sets. This means that the uniqueness of the solution is questionable. Obviously, in this case the alikeness of the reconstructed and true discharge does not give a good indication of the quality of the identified geometry. This can be explained by the nature of the DUD parameter identification procedure (section 6.4.2).

6.3.5 Case 2 based on measurements generated by TRISULA

- *Description*

The testcase described in subsection 6.3.4 shows the possibility that the identification procedure converges towards the wrong parameter-set. The question arises how it can be ensured that the true geometry is identified. The adoption of additional data from the river might be a solution. This case tests whether measurement of the width B, which is assumed to be uniform in this case, ensures identification of the true parameter-set.

Again two different runs are performed. In the first run the true value of B is not only used as a first order estimate but also kept constant during the identification. Thereafter the influence of inaccurate measurement or estimation of the width is traced. A first order estimate of B is taken that has a deviation of 10 % from the true geometry.

- *Results*

Results of this case are taken up in Appendix H. In the first place it can be concluded that the upstream discharge is identified very accurately. The numerical results show that the true value of the depth is identified. Nevertheless, the identified values of the parameters i_b and C do not coincide with the true values. Especially the identified value for the mean bottom slope is very inaccurate.

The second run of the identification procedure shows that, also when the width is estimated inaccurately, the procedure still converges towards a geometry that is comparable to the geometry identified before. But the accuracy of the identified parameter-values does, of course, not increase.

Again the identified value of the dispersion coefficient deviates in an extreme way from its input-value. In this case the ratio between the advective and the dispersive transport mechanisms, is about 1800. This means that the influence of the dispersion is small, which explains the difficulty in the identification of the value of the value of K.

It has to be concluded that measuring, or estimating, the width still does not provide the system the extra information it requires to identify the exact geometry.

6.4 CONCLUSIONS

6.4.1 About the results

Results of the test-cases show that a river geometry and an upstream discharge can be identified that yield observations that coincide with the measurements. The quality of the identified (unsteady) discharge is satisfying in all cases. Nevertheless, regarding the objective of the study, identification of the non-uniform geometry, some problems occurred.

The testcase treated in subsection 6.3.4 showed the possible identification of a parameter-set that matches the true parameter-set in no way. This can be imputed to the first order estimates of the parameter-values. These were based on expressions derived in chapter 5 and turned out to be extremely deviating from their true values.

In section 6.3.5 it has been shown that even if the width is measured, or estimated, the identified values still proportionally deviate from the true values. It has to be concluded that estimating the width still does not provide the system the information it requires to identify the exactly 'true' geometry. This means that different combinations of parameter-values exist that underlie observations that are very much alike.

Even if the identified geometry resembles the exactly 'true' geometry (subsections 6.3.2 and 6.3.3), deviations occur in the identified values from the true values in the order of magnitude of percentages. This means that, for the identification of a natural river, one can never be sure of the accuracy of the identified geometry. This imposes restrictions on the application of the results for further use. Based on the identified geometry, observations of water levels produced by a flow model under different circumstances (another flood wave; period and amplitude) will most likely differ from the measurements. In section 6.5 the prediction of water levels is discussed.

It can be concluded that the identification system is capable of identification of an unsteady discharge, whose quality is satisfying in all cases. But it is obvious that the quality of the identified discharge does not give a good indication of the identified geometry. Apparently, the number of parameters is that large that it is not possible to identify their exact values from the information that can be gained from the given measurements.

The accuracy of identified values for hydraulic and correction coefficients depends on the influence of the accessory mechanisms on the flow and transport processes. When, for example, the dispersional transport of matter is small compared to the advective transport, the accuracy of the identified value for the dispersion coefficient is small. And so, if the share of the momentum exchange in the total energy dissipation is small compared to the share of the bottom friction, the accuracy of the identified value for the entrainment coefficient is small. The identified values for these parameters should therefore be seen as indicative values.

It also has to be notified that it is not sure that, for one river section, the same geometry will be identified if the identification procedure is run twice, based on measurements taken under different circumstances.

In subsection 6.4.2 possible explanations for the behaviour of the system are given.

6.4.2 Comments on the DUD-procedure

The DUD-procedure seems to be a powerful tool in solving a problem, defined as minimizing the difference between reconstructed observations and 'true' measurements. Nevertheless some problems did occur using DUD in this study.

On the uniqueness of the solution

Problem:

- It turns out that different combinations of parameter-values exist that have no resemblance but do underlie observations that are very much alike. This means that, for the identification of a natural river, one can never be sure that the identified geometry coincides with the true geometry.

Explanation:

The DUD-procedure is a 'local optimisation method'. Best values of a parameter-vector are identified when a cost function, defined as the difference between an observation and a measurement vector, is minimized. The possibility exists that the p-dimensional manifold, spanned by values of the cost function produced by different parameter-vectors, has different local minima. Although the procedure is able to 'walk' out of the domain that is spanned by the $p+1$ first order estimates, the search of the DUD-procedure might collapse into a subplain of the parameter space (a local but not the absolute minimum is found). This means that the identified geometry matches the true geometry in no way although the quality of the produced observations is satisfying. An example of which is given in subsection 6.3.4.

On the accuracy of the identification

Problems:

- Even if a geometry is identified that resembles the true geometry, this geometry still does not exactly coincide with the true geometry, that underlies the measurements. A deviation remains in the identified values from the true values that is in the order of percentages.

- It turns out that different combinations of parameter-values exist that all have a large resemblance with the true values and underlie observations that are very much alike.

Explanation:

Since derivatives are not used the improved vector Θ_{new} is not necessarily in a "downhill" direction from the best parameter-vector so far, Θ_{p+1}. If the residue of the identification reaches a (local) minimum, it is possible that the slope of the manifold that represents the cost function (i.e. the residue) becomes very flat. This means that different combinations of parameter-values exist that have a large resemblance and produce observations that are very much alike. This results in inaccurate improvement of the parameter vector, which determines the accuracy of the identified geometry.

Further converging of the procedure and improvement of the parameter-vector can be obtained by the use of a step-shortening procedure:

$$\Theta_{new} = d\Theta_{new} + (1-d)\Theta_{p+1} \tag{6.1}$$

Where:

$$d = (0.5)^i \tag{6.2}$$

With $i = 0$ for the first ten steps in the iteration procedure, $i = 1$ for the second ten steps, and so on.

Different runs of the procedure, based on the same first order estimate but including different p parameter vector differences, converge towards the same minimum in the cost function. But because the course of the improvements of the parameter-vector is different and the true geometry is not found, the optimized parameter-vectors (i.e. geometries) are slightly different. Section 6.5 shows the influence of the difference of the results of two runs of the identification system on the prediction of water levels.

6.5 PREDICTION OF FLOOD WAVES

6.5.1 General

This case tests the influence of the accuracy of the identification on the application of the results for further use: the prediction of water levels under different circumstances. As explained in section 6.4, the result of two runs of the identification procedure may slightly differ. It was notified that the deviation of the identified parameter-vector from the 'true' vector increases when a more complicated geometry has to be identified. Than it is no surprise to notice that, in this case, the variation in the identified vectors increases as well.

For the testcase with the more-complicated geometry, described in subsection 6.3.3, water levels of a flood wave are predicted based on two identified parameter-vectors and on the 'true' vector. In Appendix H the two identified vectors are given. It has to be notified that these vector-values deviate in an extreme way.

The circumstances are different than those under which the geometries are identified. In the schedule below the data are given of the wave that is used in the identification and of the wave for which the water levels are predicted.

Wave-data:		Identification:	Water-level prediction:
T_{wave}	[s]	2000	8000
Q_{min}	[m³/s]	20.00	50.00
Q_{max}	[m³/s]	40.00	150.00

Fig.12 Wave-data from identification and prediction cases

6.5.2 Results

Resulting water levels can be found in Appendix I. The deviation in the water levels produced using the identified and the 'true' parameter-vectors is in the order of decimeters. It is obvious that this deviation decreases if the identified parameter-vectors agree better. This is the case for milder slopes, less stagnant zone and more uniform flow- and depth profiles.

6.6 APPLICATION OF THE IDENTIFICATION SYSTEM

From this we can conclude that the system is well applicable for identification of the unsteady discharge. Identification of the geometry seems to be more difficult.

It has been shown that different combinations of parameter-values may be the result of the identification. Moreover, even if the identified geometry resembles the true geometry, there always remains a deviation in the identified geometry from the true geometry. This means that one can never be sure of the accuracy of the results. Especially in mountain streams with steep slopes and large stagnant zones, one has to be cautious if the resulting, optimized, geometry is used in a flow model, for example to predict water levels under flood wave circumstances.

7 Characterization of a natural river

7.1 GENERAL

The ISMES institute at Bergamo, Italy, performed discharge measurements with the tracer methodology. Measurements were taken in the Stabina river section with the purpose to quantify a discharge under steady conditions, for evaluations related to water quality analyses. An instantaneous release of the tracer was applied. Nevertheless these measurements are used as a test-case to identify the geometry of the river section.

The water levels were not measured but are supposed to be constant during the measurement. As well the distance between the points of release and measuring was not exactly measured, but was estimated about 30 [m]. Photos are used for a first indication of the superficial width. The release consisted of 30 [l] NaCl-solution. The measurements were performed using a conductivity meter. The conductivity curve can be converted in a concentration curve using a conversion table (see Appendix J).

Data:

River	Stabina	
Section	Ponte Mulino	
Date	24 March 1995	
Water levels	unknown, though constant	[m]
NaCl-solution	30.00	[l]
Solution conductivity	124400.00	[μS/cm]
Background conductivity	109.30	[μS/cm]
Estimated distance	30.00	[m]
Estimated width	5.00	[m]

Converted:

Solution amount	3	[kg]
Background concentration	0.05	[kg/m^3]

Section 7.3 discusses the numerical identification of the geometry. The first order estimation is adjusted to steady flow conditions and to an instantaneous, in stead of continuous, release. First in section 7.2 an analytical approach is discussed. Both approaches result in an optimized parameter-vector, whose values describe the geometry of the river section. The results of the two approaches can be compared, which gives an impression of the quality of the numerical identification.

First some parameters are defined:

$$\beta = \frac{A_s}{A - A_s} = \frac{\beta_s}{1 - \beta_s} \tag{7.1}$$

$$v_c = \frac{L}{t[\max(\phi(L,t))] - t_{release}} \tag{7.2}$$

$$u = (1 + \beta) v_c \tag{7.3}$$

Where β = the ratio of the stagnant zone area relative to the area of the main stream; v_c = convective velocity of the dissolved matter [m/s]. Equation (7.3) shows a delay in the arrival time of the concentration cloud due to the presence of a stagnant zone.

7.2 ANALYTICAL APPROACH

7.2.1 Solution according to Taylor/Fischer

Because an instantaneous release was applied under steady conditions, the analytical solution given by Eq. (3.68) can be used to reconstruct the downstream concentration measurement.

$$\phi(x,t) = \frac{M/A}{2\sqrt{\pi K_x t}} \exp\left(\frac{-(x-ut)^2}{4K_x t}\right) \tag{7.4}$$

This solution is based on the one-dimensional dispersion equation according to Taylor. The expression for the longitudinal dispersion coefficient (K_x) can be used that was suggested by Fischer Eq. (3.72). The analytical solution has the character of a Gauss-curve. Conditions for using the analytical solution are a steady, uniform flow and a distance between the points of measuring and release that is that large that a linear increase of the variance σ_x^2 of the concentration-curve occurs in time, where:

$$\sigma_x^2 = 2K_x t \tag{7.5}$$

This condition is satisfied for $x > L$, where the minimum distance L is already defined by (2.4). For smaller values of x the profile of the concentration curve adapts itself to the velocity profile over the cross-section and the influence of the dispersion is negligible. In this 'convective period' skewness occurs: The concentration profile as a function of the time has a relatively steep front and a long tail.

7.2.2 Stagnant zone model

The analytical solution by Eq. (7.4) does not give a correct reconstruction of the measured downstream concentration in a natural river. These curves have a characteristic asymmetric, skewed, profile (see Fig.2), which cannot be explained by the skewness that occurs in the convective period. The main cause of this skewness has to be found in the presence of stagnant zones.

A better reconstruction of the measured concentration in a point $x=L$ can be produced by including the effects of the stagnant zone. There is no analytical solution but an improved approach can be found by means of the Edgeworth-form of the Gram-Charlier series of the Type A (Chatwin, 1980). A reasonable reconstruction of these series can be found in (Van Mazijk and Bolier, 1993):

$$\phi_E(L,t) \approx \frac{m_t}{\sqrt{2\pi\sigma_t^2}} \exp\left[-\frac{(t-\mu_t)^2}{2\sigma_t^2}\right] * \left[1 + \frac{g_t}{6\sigma_t^2} H_3\left(\frac{t-\mu_t}{\sigma_t}\right) + \ldots\right] \tag{7.6}$$

Where:
$H_3(z) = z^3 - 3z$ = third Hermiet polynomial

The moments of the approach $\phi_E(L,t)$, Eq. (7.6), equal the moments of the analytical solution $\phi(x,t)$, Eq. (7.4). Wen x is that large that the condition is satisfied that

$$x \gg \frac{K_x}{u} \tag{7.7}$$

simplified expressions can be found for the moments:

$$m_t = \int_0^T (\phi(L,t) - \phi_0)\,dt \tag{7.8}$$

$$\mu_t = \left[\frac{L}{u} + \frac{2K_x t}{u^2}\right](1+\beta) \tag{7.9}$$

$$\sigma_u^2 = \frac{2K_{xs}t}{u^2} \tag{7.10}$$

$$g_t = G_t \sigma_t^3 \tag{7.11}$$

Where:

m_t	= zero-order moment		[kgs/m^3]
μ_t	= first-order moment	= mean	[s]
σ_t^2	= second-order moment	= variance	[s^2]
g_t	= third-order moment		[s^3]

Adjusted to the system of equations used in this study, the remaining parameters are defined as:

$$K_x = \mu \frac{C}{\sqrt{g}} \frac{uB^2}{a} \tag{7.12}$$

$$P_s = B + 2a \tag{7.13}$$

$$P = \alpha_s P_s \tag{7.14}$$

$$D = \frac{P}{A_s} Eu \tag{7.15}$$

$$\omega = \frac{u}{LD} \tag{7.16}$$

$$K_{xs} = K_x \left[(1 + \beta)^2 + \frac{uL\omega B}{K_x} \right] \tag{7.17}$$

$$G_t = g_t \left(\sigma_t^2 \right)^{-\frac{3}{2}} \tag{7.18}$$

Where: P = contact-length of mean stream and stagnant zone [m]; P_s = wetted perimeter [m]; D = exchange velocity [1/s]; ω = relative stay in stagnant zone [-]; K_x = longitudinal dispersion coefficient according to Fischer [m^2/s]; K_{xs} = stagnant zone dispersion coefficient [m^2/s]; G_t = skewness-coefficient according to Abramowitz and Stegun (1965); $0 < \alpha_s < 1$ = a constant.

In the case for $\beta_s = 0$ (no stagnant zone) and $G_t = 0$ (no skewness), the series approach produces a concentration curve identical to the analytical solution in the point $x = L$.

7.2.3 Results of the identification

The stagnant zone model is used to identify the river geometry. Although not all the parameters of the numerical identification system are included in the series-approach, it gives reasonable comparable results.

Appendix J shows the identified downstream concentration that gives the best approach of the measurement. The analytical solution after Taylor/Fischer has been plotted in the same figure for the same parameter values. It is obvious that the series-approach gives a better approach of the measured curve than the analytical solution of the Taylor model. The schedule summarizes the values of the identified parameter-vector. We notice that the value for the stagnant zone coefficient is small. The results are compared with the numerical identification in section 7.4.

Using equation (7.3) a value for the flow velocity u is found. A value for the steady discharge can be found when the identified values of the depth a and the width B are used. This value of the discharge can be compared with the value identified by the numerical system.

u	$= 0.163$	[m/s]	by (7.3)
Q	$= 0.765$	[m³/s]	$= u \cdot a \cdot B \cdot (1-\beta_s)$

By means of the identified geometry it is possible to verify if condition (7.7), that imposed a restriction on the use of the simplified expressions for the moments, was indeed fulfilled. Substitution of the identified parameter-values in equations (7.7) and (7.12) yields the condition $x \gg 0.53$ [m], which is fulfilled by the distance of 30 [m].

7.3 NUMERICAL APPROACH

7.3.1 First order estimation

Estimates of the values of the system parameters, needed to run the numerical model, are now based on steady-flow conditions and an instantaneous release of the tracer. Following expressions are used to gain first estimates of the parameter-values:

$$Q_s = \frac{M}{\int_0^T (\phi(L,t) - \phi_0)\,dt} \tag{7.19}$$

$$A_s = \frac{Q_s}{u} \tag{7.20}$$

$$a = \frac{A_s}{B} \tag{7.21}$$

$$i_b = \frac{u^2}{C^2 a} \tag{7.22}$$

Q_s and A_s are the steady state values of the discharge and the cross sectional area. Values for the coefficients μ, β_a, β_s, f and fE are defined as in section 5.2 (equations (5.30) through (5.35)). Based on photographs, the following assumptions are made:

$$B_{up} = B_{down} = B = 5 \tag{7.23}$$

$$C = 30 \tag{7.24}$$

7.3.2 Results of the identification

The identification system, described in chapter 5, is adapted to the expressions given above. Identification results in a geometry of the river section and a steady discharge that underlie the observation of a downstream concentration curve that has a good resemblance with the measured curve (Appendix J). Parameter values of the identified geometry are summarized in the schedule. It can be noticed that, again, the identified value for the stagnant zone coefficient β_s is small.

An additional result of the identification is the steady discharge:
Q_s = 0.58 [m^3/s].

7.4 COMPARISON OF IDENTIFICATIONS

The results of the numerical identification system and the best reconstruction by the series-approach can be compared. In Appendix J the graphical and numerical results are summarized. In the first place we notice that the reconstructed concentration curves look very much alike. The identified steady discharges Q_s differ slightly but have the same order of magnitude (analytical: 0.76; numerical: 0.58 [m^3/s]).

It can be noticed that both the numerical and the series-approach identify a relatively small stagnant zone coefficient. This can be explained by the short distance between measuring point and point of release. On this short interval there is a limited exchange of tracer-substance between stagnant zone and main stream. This causes only a small delay in the downstream arrival time of the concentration cloud and has limited influence on the skewness of the concentration curve.

It has to be notified that the value of β_s for the numerical approach is based on the identified value for σ_u, which also contains the effects of the non-uniform distribution of the depth and flow profiles.

The analytical, series-approach, is based on a uniform width. The numerical identification system on the other hand, identifies a narrowing width that agrees reasonably with this uniform width. Also the identified values for the dispersion coefficient μ agree well.

Larger deviations occur in the identified values for the Chézy-coefficient C, the depth a and the bottom slope i_b. A possible explanation is that the bottom slope for the analytical solution is not a direct result of the computation but was calculated using the Chézy-formula Eq. (7.22) and the identified value for the flow velocity u Eq. (7.3).

The largest deviations occur in the values for the coefficients f and E. Before a coefficient fE (representing $f \cdot E$) was used in stead of the entrainment coefficient E. Now it is possible to compare the numerical with the analytical value for the entrainment coefficient, using Eq. (7.15). These large deviations may be explained by the nature of the series-approach, which is entirely different than the numerical model. As concluded before (chapter 6), the parameter f only ones occurs independent a term of the transport equations, which explains its limited influence. Moreover, identification of this value is not important regarding the use of the results in a flow model. The deviation in the identified values for E may be explained by the contribution of the exchange term to the total energy dissipation Eq. (3.30), which is negligible with respect to the contribution of the frictional effects (a large bottom roughness is identified: $C = 30$ [$m^{1/2}/s$]). Because E only occurs in this exchange term, its influence on the flow processes is limited.

Because the correction coefficient β_a is not included in the series-approach, it is not possible to compare the value identified by the numerical identification system.

The identified values for the geometrical parameters (Schedule) give a reasonable indication of the geometry of the Stabina river section. The values can be used to simplify the river section. The correction coefficients give a first indication of the non-uniformity of the flow over the cross-section.

8 Conclusions and recommendations

8.1 CONCLUSIONS

- **Objective and approach**

The objective is the characterization of the non-uniform geometry of a mountain river and the development of a method that enables identification of this geometry of a particular river section. Identification of the geometry enables simplification in modelling, which can be applied in a wide range of applications.

Identification is based on the tracer methodology, which means that a non-disintegrating substance is released upstream of a river section and water levels and concentrations are continuously measured. Therefore attention has been paid to the flow and transport processes in a mountain stream with irregular geometry. A flow and transport simulating numerical model is developed. Integrated with the parameter identification system DUD, this system identifies the geometry that yields observations that coincide with the measurements. An additional result is the reconstruction of the upstream, unsteady, discharge.

- **On the results of the characterization of an irregular geometry**

Results of the test-cases show that the system is able to identify a river geometry and an upstream discharge yielding observations that coincide with the measurements.

Besides values for the geometry-related parameters, values are identified for hydraulic and correction coefficients. The identified value for the coefficient σ_u corrects the influence of the non-uniformity of the flow and depth profiles over the cross-section on the flow processes. A coupling of the use of correction coefficients and the stagnant zone concept enables rewriting of σ_u into a coefficient β_s, representing a ratio of stagnant zones relative to the total cross section. The identified value of β_a merely indicates the non-uniformity of the depth over the width of the stream. Identified values of the parameters fE and μ represent an over-all entrainment coefficient for the exchange of momentum and matter and a dispersion coefficient. These values may be applied in transport models. The parameter f indicates the fraction of stagnant zones on the river length L.

- **General restrictions of the system**

The flow model is only applicable in flows with moderate Froude numbers. A further limitation is that the model is not capable of handling internal transitions between subcritical and supercritical flow.

While identification is based on fitting observed and measured concentration *curves*, the system is applicable in two different situations. The first situation is the continuous release of a tracer substance for sufficiently long time. A concentration curve is obtained when a flood wave enters the river section with equilibrium downstream concentration. A second possibility is the instantaneous release of a tracer substance in steady flow conditions.

- **On the applicability of the identification system**

It can be concluded that the system is well applicable for the identification of an unsteady discharge. Regarding the objective of the study, the identification of the geometry, some problems occurred.

On the uniqueness of the solution:

It turns out that different combinations of parameter-values exist that have no resemblance but do underlie observations that are very much alike. This means that a geometry can be identified that matches the true geometry in no way although the quality of the reconstructed observations and unsteady discharge satisfies. For the identification of a natural river one can never be sure that the identified geometry coincides with the true geometry.

On the accuracy of the identification:

Even if a geometry is identified that resembles the true geometry, this geometry still does not exactly coincide with the true geometry, that underlies the measurements. A deviation remains in the identified values from the true values that is in the order of percentages.

On the identification of hydraulic and correction coefficients:

The accuracy of identified values for hydraulic and correction coefficients depends on the influence of the accessory mechanisms on the flow and transport processes. When, for example, the dispersional transport of matter is small compared to the advective transport, the accuracy of the identified value for the dispersion coefficient is small. And so, if the share of the momentum exchange in the total energy dissipation is small compared to the share of the bottom friction, the accuracy in the identified value for the entrainment coefficient is small. The identified values for these parameters should therefore merely be taken as indicative.

8.2 Recommendations

Improvement of the results:

- Further converging of the procedure and improvement of the parameter-vector can be obtained by the use of a step-shortening procedure.

- Another possibility is the identification in two steps: first identification of the geometrical parameters, than identification of the hydraulic and correction coefficients.

On the application of the identification system:

- The system is very well capable of identification of an unsteady discharge. The accuracy of the identified discharge satisfies in all test-cases.

- The system is capable of identification of a geometry that underlies observations that coincide with the measurements of the dilution method. The accuracy of the identified geometry determines the applicability of the results for further use.

  It has been shown that the exact geometry is never identified. Moreover, the uniqueness of the solution is questionable. This means that one has to be cautious if the identified geometry is used to simplify the studied river section. Observations of water levels produced by a flow model under different circumstances (another flood wave; period and amplitude) will most likely differ from the measurements.

Enlargement the applicability of the system:

- The restrictions that are put on the identification system are most likely due to the nature of the used parameter-identification system, DUD: ***Doesn't Use Derivatives***. Improvement of the accuracy of the identified geometry will most likely be obtained by the use of an other identification system that is based on the determination of the influence of each parameter on each observation. Be aware that these methods are significant time and memory consuming.

- The applicability of the system will be enlarged when the flow model is enabled to handle supercritical flow and internal transitions.

Recommendations for further study:

- Field measurements are recommended to investigate the applicability of the identification system. While the uniqueness of the solution is questionable, it may be interesting to investigate the accuracy of water level predictions based on different identified parameter-sets.

- Another question that remains is if, for one section of a natural river, the same geometry is identified if the identification system is run twice based on performance of the dilution method under different circumstances.

Symbols

Symbol		*Description*	*Dimension*
a		river depth over the width	[L]
$\bar{a}$		mean depth	[L]
a_{ms}		river depth in main stream	[L]
a_0		first order estimate of the river depth	[L]
A		cross-sectional area	[L^2]
A_s		cross-sectional area of the stagnant zones	[L^2]
B		width of the river	[L]
B_{ms}		width of the main stream	[L]
B_{down}		width at downstream measuring point	[L]
B_{up}		width at upstream measuring point	[L]
c		characteristic celerity of small disturbances	[LT^{-1}]
		flood wave propagation speed	[LT^{-1}]
c_r		ratio of analytical and numerical flood wave celerity	[-]
C		Chézy friction coefficient	[$L^{½}T^{-1}$]
d_n		relative numerical damping factor	[-]
D		exchange velocity	[T^{-1}]
E		entrainment coefficient between mainstream and stagnant zone	[-]
f		fraction of stagnant zones on length L	[-]
f_x		time and depth averaged mass flux in longitudinal direction	[$ML^{-2}T^{-1}$]
f_y		time and depth averaged mass flux in transversal direction	[$ML^{-2}T^{-1}$]
f_ϕ		mass-flux between main stream and stagnant zones	[$ML^{-3}T^{-1}$]
$f(\Theta)$		system evaluation, observation vector	[-]
Fr		Froude number $= u/\sqrt{(g \cdot a)}$	[-]
g		gravitation constant	[LT^{-2}]
g_j		acceleration due to gravity in j-direction	[LT^{-2}]
g_t		third-order moment	[T^3]
G_t		skewness-coefficient according to Abramowitz and Stegun	[-]
h		water level	[L]
i_b		average bottom slope	[-]
j		space step number	[-]
$J(\Theta)$		cost function of system evaluation	[-]
k		wave number $2\pi/L$	[rad $\cdot$ T^{-1}]
K_x	$= K$	longitudinal dispersion coefficient	[L^2T^{-1}]
K_{xs}		stagnant zone dispersion coefficient	[L^2T^{-1}]
K_y		transversal dispersion coefficient	[L^2T^{-1}]
K_{num}		numerical diffusion coefficient	[L^2T^{-1}]

Symbol	*Description*	*Dimension*
$l(\alpha)$	linear approximation of $f(\Theta)$	[-]
L	length of the river section	[L]
	length of flood wave	[L]
	length of concentration cloud	[L]
m_t	zero-order moment	$[MT \cdot L^{-3}]$
M	tracer release	$[MT^{-1}]$
n	number of elements in Y and $f(\Theta)$	[-]
	time step number	[-]
p	pressure	$[ML^{-1}T^{-2}]$
	number of parameters in parameter vector Θ	[-]
p''	fluctuation in pressure due to turbulence	$[ML^{-1}T^{-2}]$
P	wetted perimeter	[L]
	Cell Péclet number	[-]
	contact-length of mean stream and stagnant zone	[L]
P_s	wetted perimeter	[L]
Q	river discharge	$[L^3T^{-1}]$
Q_m	'measured' discharge using steady state formula	$[L^3T^{-1}]$
T	flood wave period	[T]
u	cross sectionally averaged velocity	$[LT^{-1}]$
	time-averaged velocity-component in flow direction ($\bar{u}+u'$)	$[LT^{-1}]$
$\bar{u}$	depth-averaged velocity-component in flow direction	$[LT^{-1}]$
	cross-sectionally averaged velocity-component in flow direction	$[LT^{-1}]$
u'	time-averaged local deviation of the depth averaged velocity $\bar{u}$	$[LT^{-1}]$
u''	fluctuation in longitudinal velocity due to turbulence	$[LT^{-1}]$
U	total velocity-component in flow direction	$[LT^{-1}]$
u_{max}	maximum flow velocity during flood wave	$[LT^{-1}]$
u_{ms}	velocity in the main stream	$[LT^{-1}]$
u_*	friction velocity	$[LT^{-1}]$
v	velocity component in direction perpendicular to flow ($v+v'$)	$[LT^{-1}]$
v	depth-averaged velocity	$[LT^{-1}]$
v'	time-averaged local deviation of the depth averaged velocity v	$[LT^{-1}]$
v''	fluctuation in transversal velocity due to turbulence	$[LT^{-1}]$
v_c	convective velocity of the dissolved matter	$[LT^{-1}]$
V	total velocity-component in transversal direction	$[LT^{-1}]$
w	vertical flow velocity	$[LT^{-1}]$
w''	fluctuation in vertical velocity due to turbulence	$[LT^{-1}]$
W	total velocity-component in vertical direction	$[LT^{-1}]$
Y	vector containing the measurements	[-]
z_b	bottom level	[L]
z_{down}	bed level in downstream measuring point	[L]
z_{up}	bed level in upstream measuring point	[L]

Symbol	*Description*	*Dimension*
α	solution vector in identification procedure	[-]
α_u	coefficient correcting the distribution of u over the cross-section	[-]
α_ϕ	coefficient correcting the distribution of ϕ over the cross-section	[-]
β	the ratio of the stagnant zone area relative to the area of the main stream	[-]
β_a	coefficient correcting the non-uniform distribution of $a \cdot a$	[-]
β_u	coefficient correcting the distribution of u^2 over the cross-section: momentum or Boussinesq coefficient	[-]
β_s	stagnant zone area relative to cross-sectional area	[-]
β_ϕ	coefficient correcting the distribution of $\phi \cdot u$ over the cross-section:	[-]
Δx	numerical space step	[L]
Δt	numerical time step	[L]
ϵ_u	hypothetical distortion of the time-mean value of the velocity from the time and cross-sectionally averaged value	[LT^{-1}]
ϵ_ϕ	hypothetical distortion of the time-mean value of the concentration from the time and cross-sectionally averaged value	[ML^{-3}]
ϵ_a	hypothetical distortion of the depth a from the mean depth $\bar{a}$	[L]
θ	numerical weighing factor	[-]
Θ	vector containing the parameters to be identified	[-]
μ	empirical factor in dispersion coefficient	[-]
μ_t	first-order moment = mean	[T]
ξ	relative grid size	[-]
Ξ	ratio of exchange effects and inertial effects	[-]
ν	kinematic viscosity	[L^2T^{-1}]
ρ	density of the water	[ML^{-3}]
	numerical amplification factor	[-]
σ	Courant number	[-]
σ_t^2	second-order moment = variance	[T^2]
σ_u	correction coefficient	[-]
τ_{ij}	shear stress in i,j-plane of water particle	[$ML^{-1}T^{-2}$]
τ_b	average bottom shear stress	[$ML^{-1}T^{-2}$]
ϕ	average concentration in main stream	[ML^{-3}]
ϕ_e	equilibrium concentration	[ML^{-3}]
ϕ_s	average concentration in stagnant zone	[ML^{-3}]
ϕ_0	natural background concentration	[ML^{-3}]
ω	$2\pi/T$	[rad $\cdot$ T^{-1}]
ω	relative stay in stagnant zone	[-]
Ω	ratio of frictional and inertial effects	[-]

References

Abbot, M.B. and D.R Basco (1989)
Computational fluid dynamics, An introduction for engineers
Longman, Harlow

Jansen, P. Ph.; L. van Bendegom; J. van den Berg; M. de Vries and A. Zanen (1979)
Principles of river engineering
Pitman, London

MathWorks Inc. (1995)
The student edition of MATLAB, version 4, User's Guide
MathWorks Inc., Prentice Hall Inc, California

Mazijk, A. van & G. Bolier (1993)
Waterkwaliteitsmodellering oppervlaktewater
(lecture notes n11)
TU Delft, Faculty of Civil Engineering

Meijer, D.G. (1992)
Dilution Method for Measurements of Unsteady Discharges in Mountain Streams
TU Delft, Faculty of Civil Engineering

Ralston, M.L. and R.I. Jennrich (1978)
DUD, a derivative free algorithm for nonlinear least squares
Journal of Fluid Mechanics, vol.16, no.1

Sieben, A. (1993)
Hydraulics and morphology of mountain rivers: a literature survey
Communications on hydraulic and geotechnical engineering
Report No. 93 - 4
TU Delft, Faculty of Civil Engineering

Sieben, A. (1995)
Personal communication

Stelling, G.S. and N. Booij (1994)
Computational modelling in open channel hydraulics
(lecture notes b84)
TU Delft, Faculty of Civil Engineering

Verspuy, C. (1987)
Lange golven (lecture notes b73)
TU Delft, Faculty of Civil Engineering

Vreugdenhil, C.B. (1989)
Computational Hydraulics, an introduction
Springer Verlag, Berlin

Vries, M. de (1993)
River Engineering (lecture notes f10)
TU Delft, Faculty of Civil Engineering

Vries, M. de (1993)
Use of models for river problems
Studies and reports in hydrology, No. 51
UNESCO publishing, United Nations, Paris

Vries, M. de & Z.B. Wang (1995)
Applied Mathematics for the Aquatic Environment
BUT-DUT University Linkage Project in the field of Water Resources Engineering
TU Delft, Faculty of Civil Engineering, Centre for International Cooperation and Appropriate Technology (CICAT)

Appendix

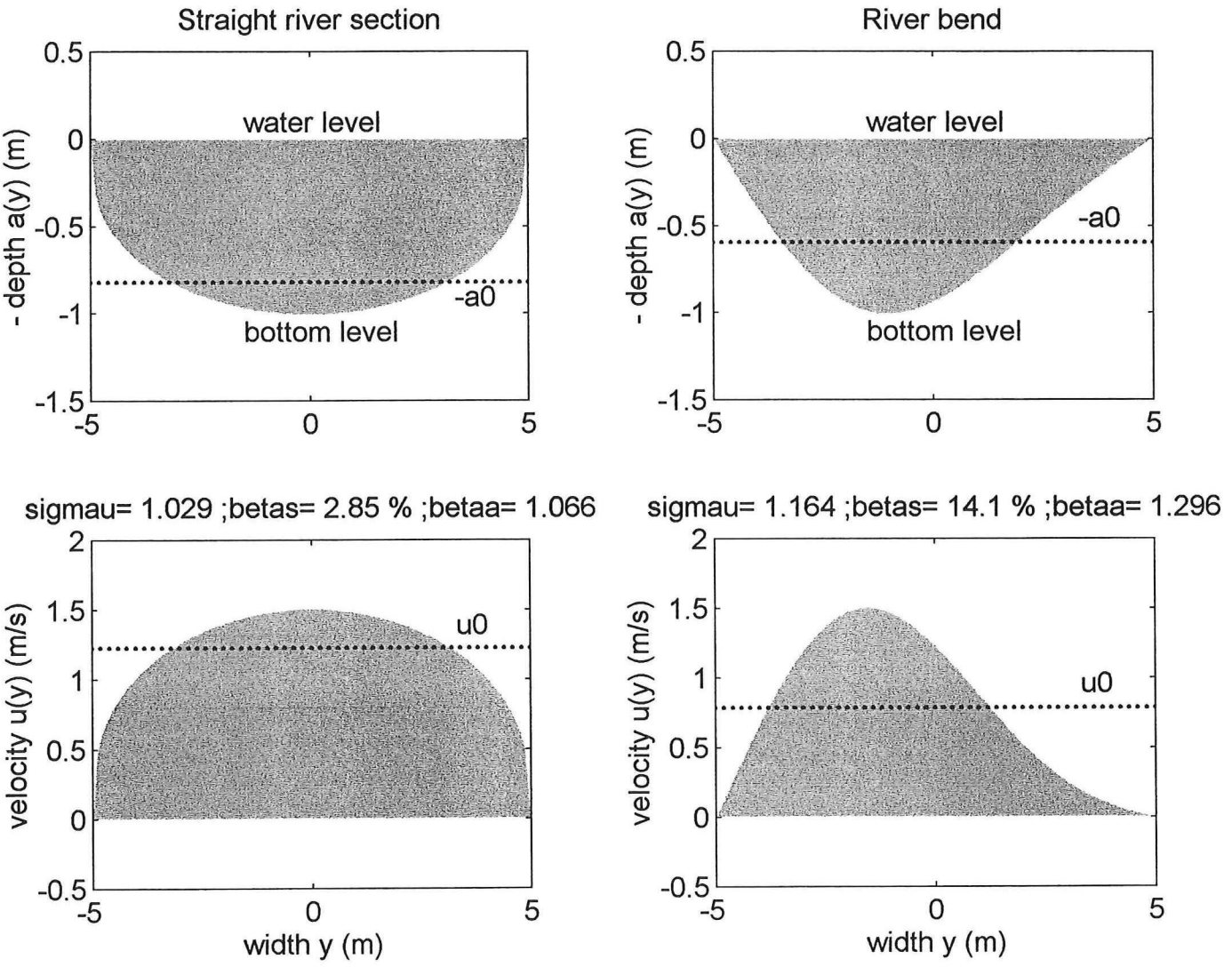
Straight river section
River bend
water level
bottom level
-a0
- depth a(y) (m)
sigmau= 1.029 ;betas= 2.85 % ;betaa= 1.066
sigmau= 1.164 ;betas= 14.1 % ;betaa= 1.296
u0
velocity u(y) (m/s)
width y (m)

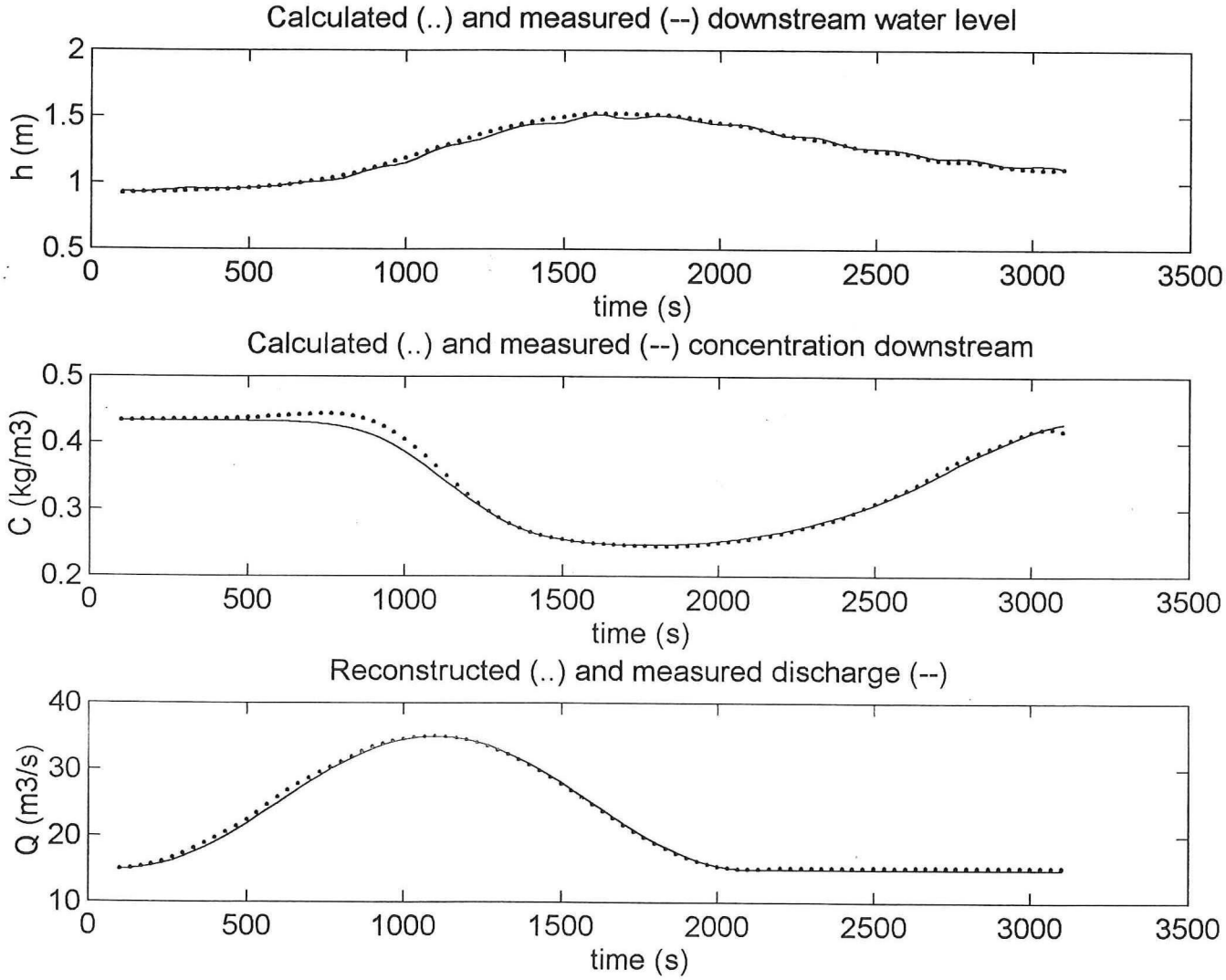
Calculated (..) and measured (--) downstream water level
h (m)
2
1.5
1
0.5
0
500
1000
1500
2000
2500
3000
3500
time (s)
Calculated (..) and measured (--) concentration downstream
C (kg/m3)
0.5
0.4
0.3
0.2
0
500
1000
1500
2000
2500
3000
3500
time (s)
Reconstructed (..) and measured discharge (--)
Q (m3/s)
40
30
20
10
0
500
1000
1500
2000
2500
3000
3500
time (s)

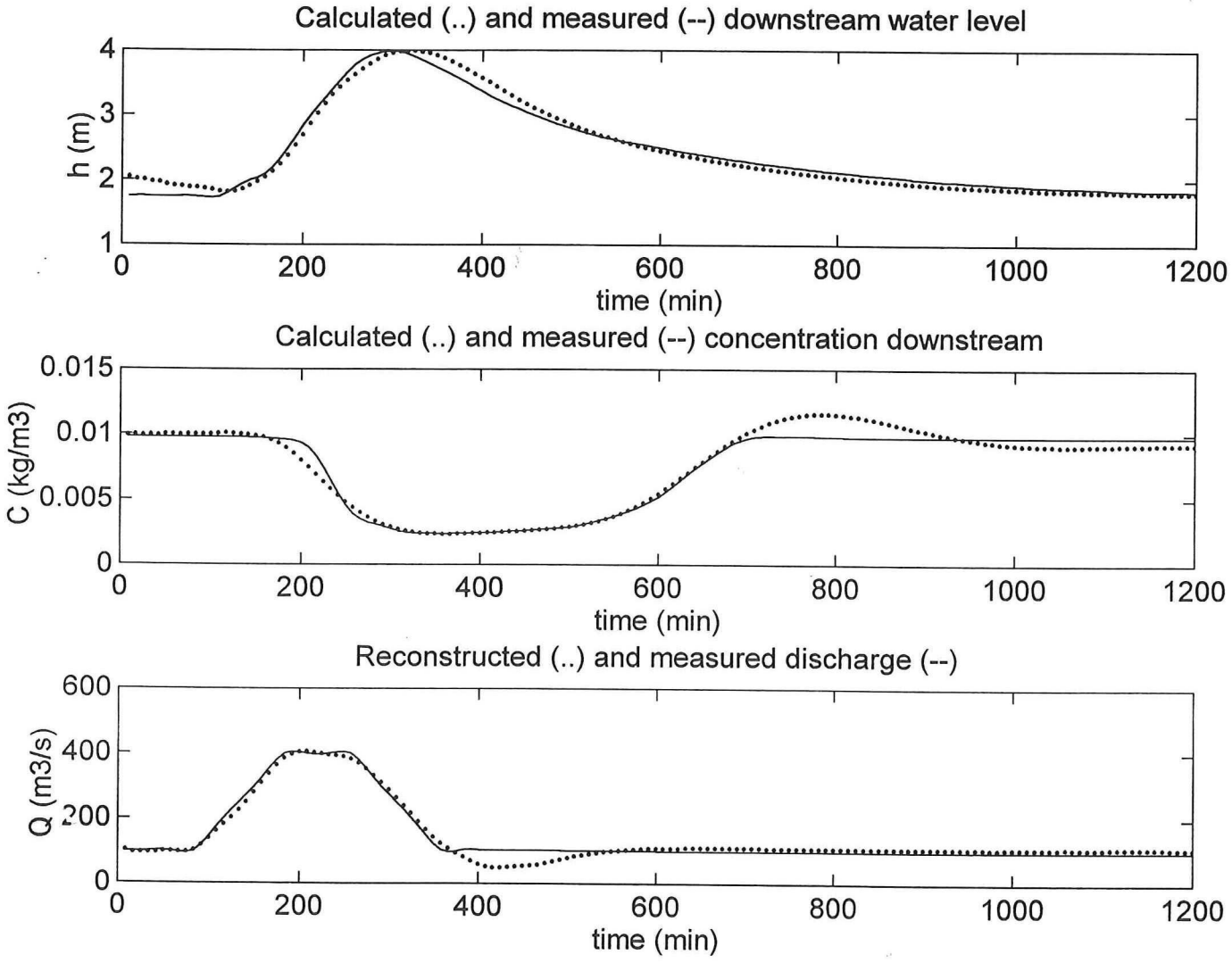
Calculated (..) and measured (--) downstream water level
h (m)
time (min)
Calculated (..) and measured (--) concentration downstream
C (kg/m3)
time (min)
Reconstructed (..) and measured discharge (--)
Q (m3/s)
time (min)

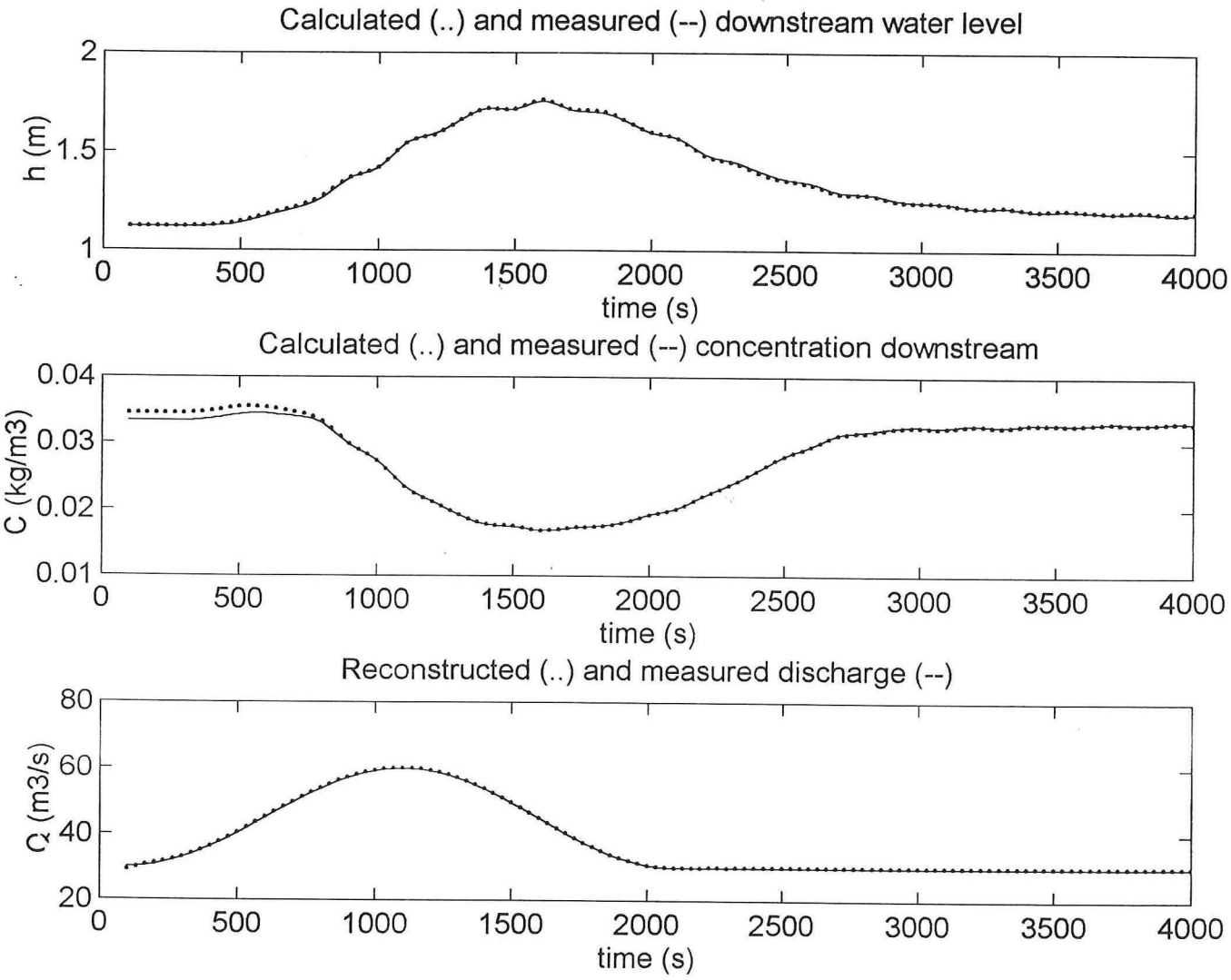
Calculated (..) and measured (--) downstream water level
h (m)
2
1.5
1
0
500
1000
1500
2000
2500
3000
3500
4000
time (s)
Calculated (..) and measured (--) concentration downstream
C (kg/m3)
0.04
0.03
0.02
0.01
0
500
1000
1500
2000
2500
3000
3500
4000
time (s)
Reconstructed (..) and measured discharge (--)
Q (m3/s)
80
60
40
20
0
500
1000
1500
2000
2500
3000
3500
4000
time (s)

Results testcase 1 based on Simulate

Subsection 6.3.2			INPUT	RESULTS	Deviation (%)
Geometry	B_{up}	[m]	20.00	20.18	0.90
	B_{down}	[m]	20.00	20.36	1.80
	i_b	[-]	$10.00*10^{-4}$	$9.77*10^{-4}$	2.30
	C	[$m^{1/2}/s$]	40.00	39.54	1.15
	a	[m]	1.1200	1.1245	0.40
Hydraulic	fE	[-]	$5.00*10^{-3}$	$5.25*10^{-3}$	5.00
	f	[-]	$1.00*10^{-2}$	$1.12*10^{-2}$	12.00
	σ_u	[-]	1.100	1.087	1.18
	β_a	[-]	1.300	1.262	2.94
	μ	[-]	$5.00*10^{-3}$	$4.84*10^{-3}$	3.20
Data:	T_{wave}	[s]	2000		
	L_{river}	[m]	1000		
	Q_{min}	[m^3/s]	30.00		
	Q_{max}	[m^3/s]	60.00		
	M	[kg/s]	1.00		
	ϕ_0	[kg/m^3]	0.00		

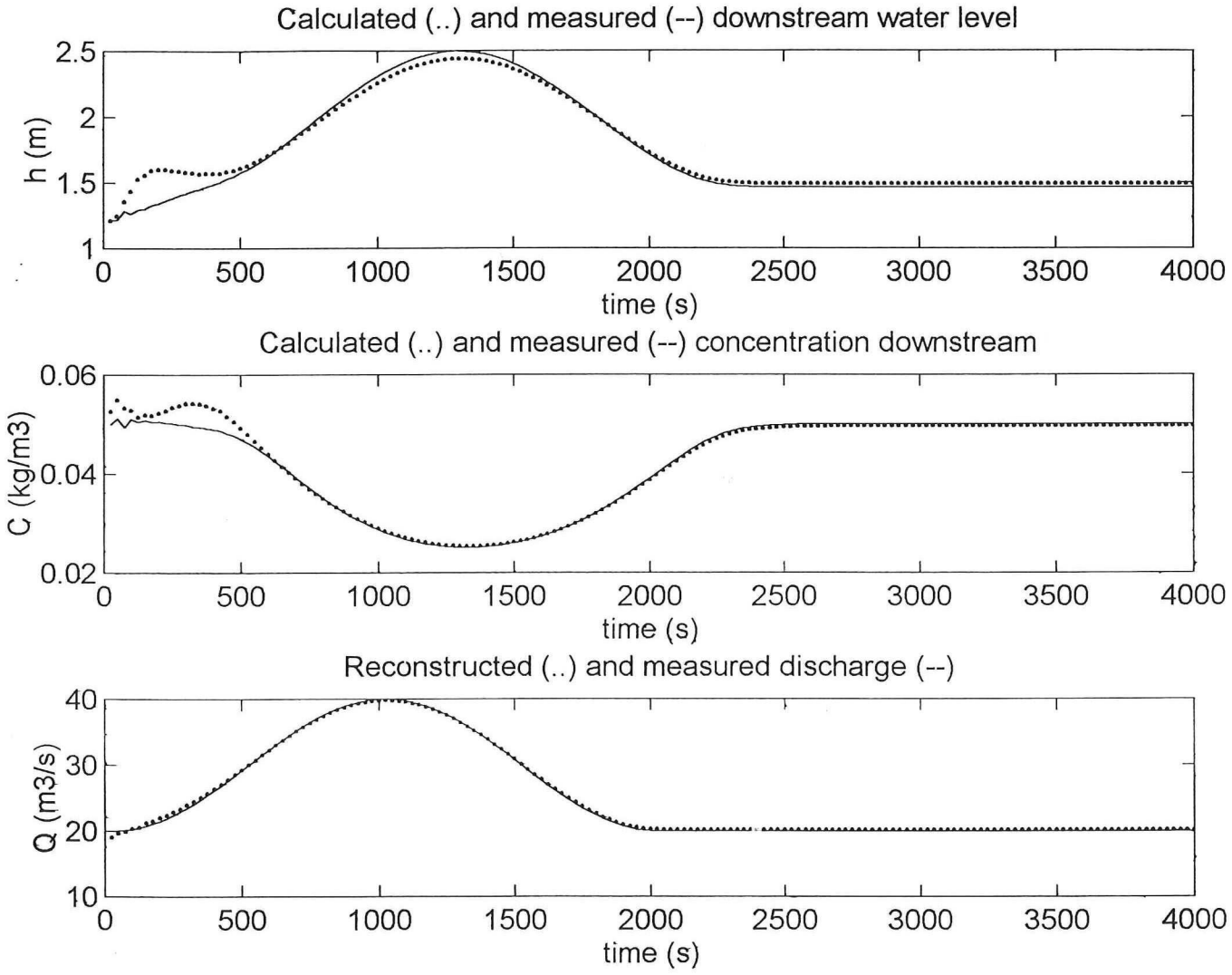
Calculated (..) and measured (--) downstream water level
h (m)
2.5
2
1.5
1
0
500
1000
1500
2000
2500
3000
3500
4000
time (s)
Calculated (..) and measured (--) concentration downstream
C (kg/m3)
0.06
0.04
0.02
0
500
1000
1500
2000
2500
3000
3500
4000
time (s)
Reconstructed (..) and measured discharge (--)
Q (m3/s)
40
30
20
10
0
500
1000
1500
2000
2500
3000
3500
4000
time (s)

Results testcase 2 based on Simulate

Subsection 6.3.3			INPUT	RESULTS	Deviation (%)
Geometry	B_{up}	[m]	10.00	9.87	1.30
	B_{down}	[m]	5.00	5.32	6.40
	i_b	[-]	$10.00*10^{-3}$	$9.89*10^{-3}$	1.10
	C	[$m^{1/2}/s$]	30.00	29.71	0.97
	a	[m]	1.4650	1.5611	6.56
Hydraulic	fE	[-]	$1.00*10^{-2}$	$1.16*10^{-2}$	16.00
	f	[-]	$1.00*10^{-1}$	$3.36*10^{-1}$	236.00
	σ_u	[-]	1.100	1.075	2.27
	β_a	[-]	1.150	1.114	3.13
	μ	[-]	$10.00*10^{-2}$	$9.66*10^{-2}$	3.40
Data:	T_{wave}	[s]	2000		
	L_{river}	[m]	1000		
	Q_{min}	[m^3/s]	20.00		
	Q_{max}	[m^3/s]	40.00		
	M	[kg/s]	1.00		
	ϕ_0	[kg/m^3]	0.00		

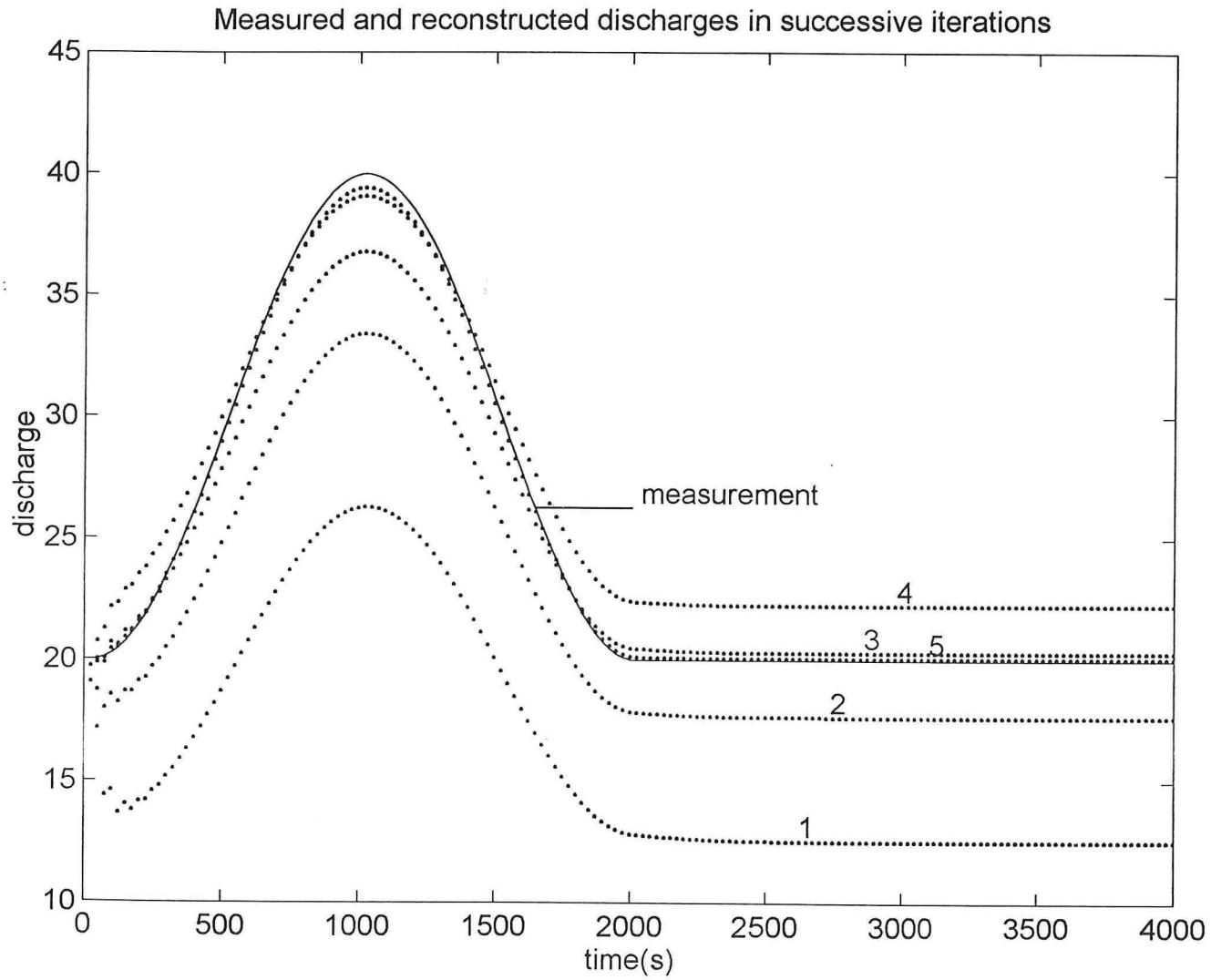
Measured and reconstructed discharges in successive iterations
discharge
time(s)
measurement
1
2
3
4
5
45
40
35
30
25
20
15
10
0
500
1000
1500
2000
2500
3000
3500
4000

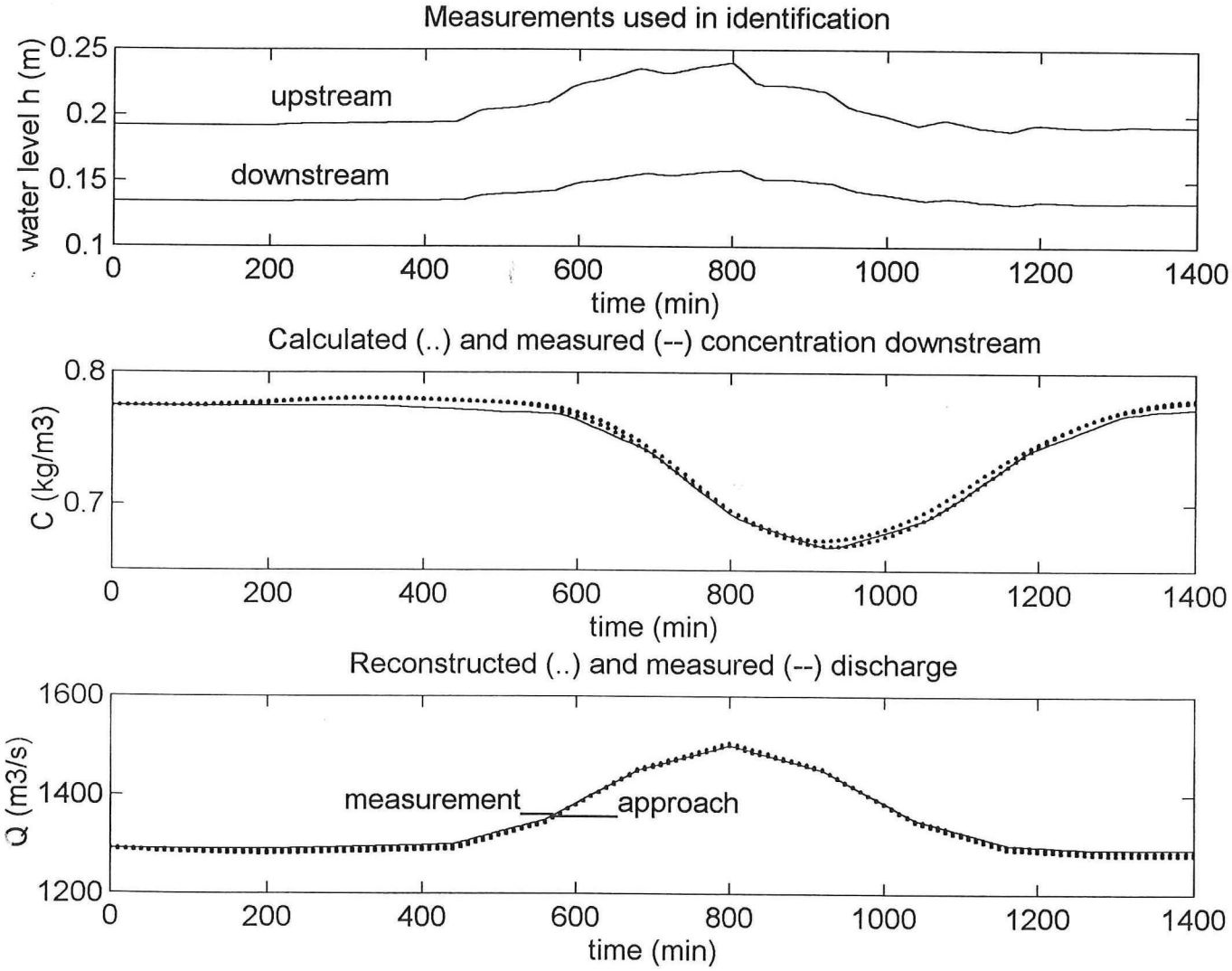
Measurements used in identification
water level h (m)
0.25
0.2
0.15
0.1
upstream
downstream
0
200
400
600
800
1000
1200
1400
time (min)
Calculated (..) and measured (--) concentration downstream
C (kg/m3)
0.8
0.7
0
200
400
600
800
1000
1200
1400
time (min)
Reconstructed (..) and measured (--) discharge
Q (m3/s)
1600
1400
1200
measurement
approach
0
200
400
600
800
1000
1200
1400
time (min)

Results testcase 1 based on TRISULA

Subsection 6.3.4		INPUT TRISULA	RESULTS 2nd run	Deviation (%)	RESULTS 1st run
Geometry	B_{up} [m]	129.00	134.26	4.07	182.25
	B_{down} [m]	129.00	131.76	2.14	193.24
	i_b [-]	$2.95*10^{-5}$	$3.39*10^{-5}$	14.92	$7.31*10^{-6}$
	C [$m^{1/2}/s$]	100.00	103.55	3.55	155.60
	a [m]	11.00	11.05	0.45	6.98
Hydraulic	fE [-]	0.00	$7.76*10^{-5}$	(**)	$2.26*10^{-4}$
	f [-]	1.00	$9.97*10^{-2}$	90.0	$1.26*10^{-2}$
	β_a [-]	1.00	1.0141	1.14	1.0084
	K [-]	10.00	501	4900	423
Stagnant zone	β_s [-]	0.00	0.0108 (*)	(**)	0.2565(*)
Data:	L_{river} [m]	7965			
	M [kg/s]	1000			
	ϕ_0 [kg/m^3]	0.00			

Remarks:

The first run is based on first order estimates for the parameter-values calculated from the expressions derived in section 5.2. First order estimates used in the second run are based on the true geometry, including arbitrary deviations.

$$K = \mu \frac{C}{\sqrt{g_z}} \frac{uB^2}{a}$$

(*) The identified value for σ_u is rewritten into a value for the parameter β_s.
(**) Impossible to compare in terms of percentages.

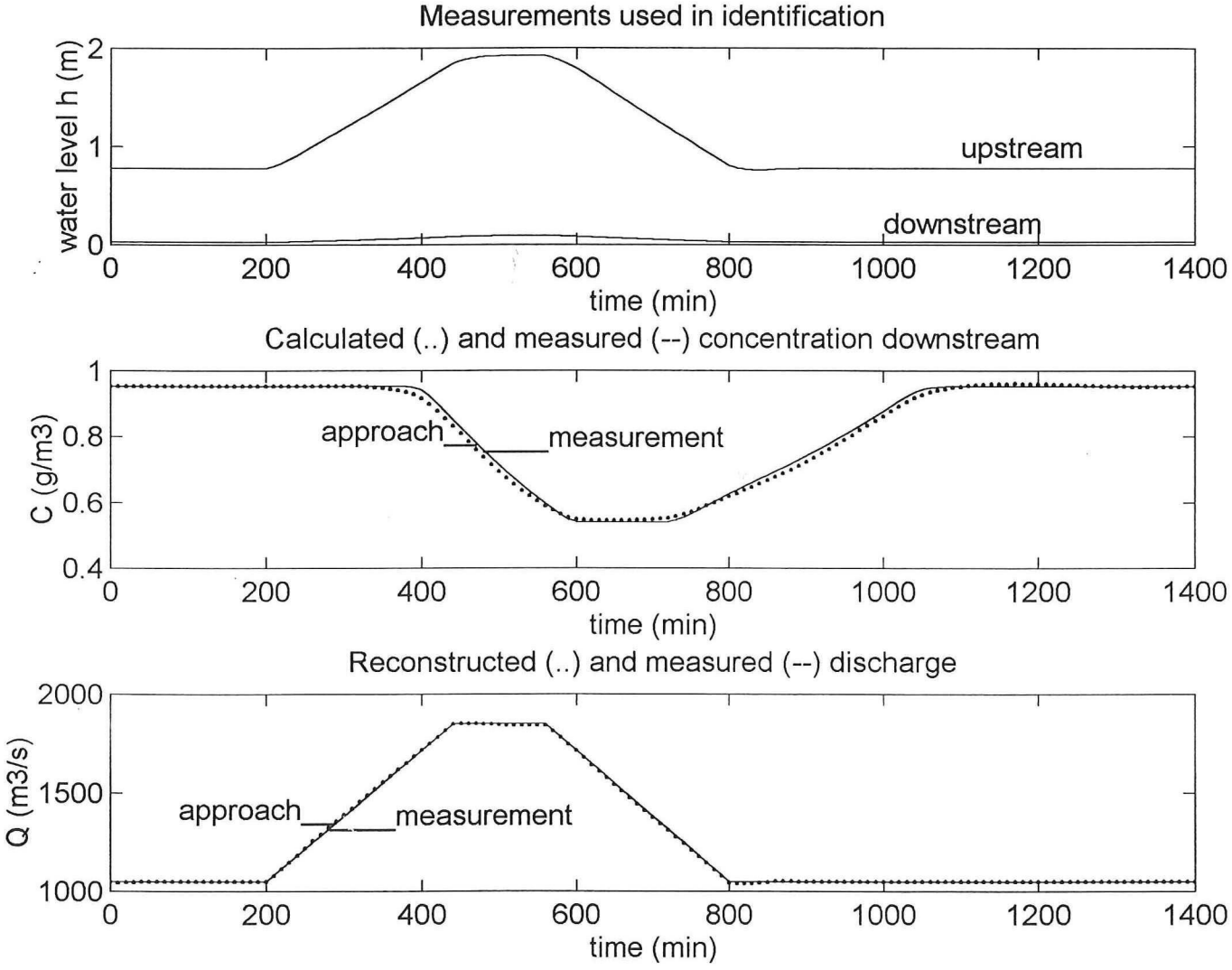
Measurements used in identification
water level h (m)
upstream
downstream
time (min)
Calculated (..) and measured (--) concentration downstream
C (g/m3)
approach
measurement
time (min)
Reconstructed (..) and measured (--) discharge
Q (m3/s)
approach
measurement
time (min)

Results testcase 2 based on TRISULA

Subsection 6.3.5			INPUT TRISULA	*B* correctly measured (150 m)	Deviation (%)	Uncorrect measured *B* (135 m)
Geometry	B	[m]	150.00	150.00	*B* given	152.31
	i_b	[-]	$2.31*10^{-5}$	$6.66*10^{-5}$	190 !	$4.97*10^{-5}$
	C	[$m^{1/2}/s$]	50.00	52.41	4.82	53.33
	a	[m]	7.00	7.04	0.57	6.828
Hydraulic	fE	[-]	0.00	$7.68*10^{-5}$	(**)	$3.25*10^{-4}$
	f	[-]	1.00	$4.06*10^{-1}$	59.4	$8.12*10^{-2}$
	β_a	[-]	1.00	1.00	0.00	1.00
	K	[-]	20	94.76	375	86.25
Stagnant zone	β_s	[-]	0.00	0.00 (*)	(**)	0.00 (*)
Data:	L_{river}	[m]	14400			
	M	[g/s]	1000			
	ϕ_0	[g/m^3]	0.0			

Results of the identification depicted in the first column are based correct measurement of the width. The second column summarizes the results of identification of the complete geometry, including the width. The first order estimation of *B* may be based on inaccurate measurement or estimation.

(*) The identified value for σ_u is rewritten into a value for the parameter β_s.
(**) Impossible to compare in terms of percentages.

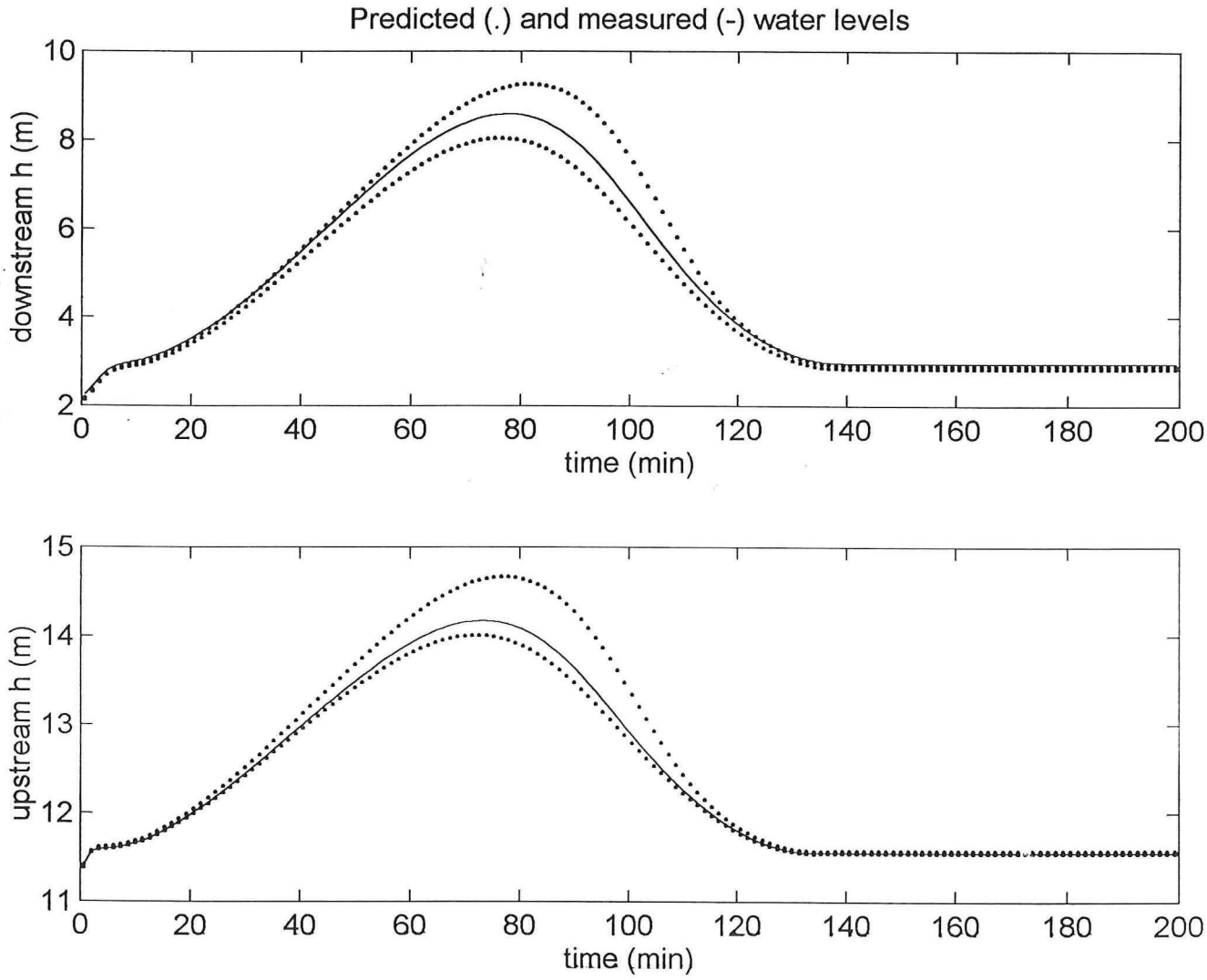
Predicted (.) and measured (-) water levels
downstream h (m)
time (min)
upstream h (m)
time (min)

Optimized parameter-sets underlying the flood-wave prediction

Section 6.5			INPUT A:	INPUT B:
Geometry	B_{up}	[m]	9.87	9.376
	B_{down}	[m]	5.32	5.23
	i_b	[-]	$9.89*10^{-3}$	$9.93*10^{-3}$
	C	[$m^{1/2}/s$]	29.71	31.41
	a	[m]	1.561	1.488
Hydraulic	fE	[-]	$1.16*10^{-2}$	$1.03*10^{-2}$
	f	[-]	$33.60*10^{-2}$	$8.65*10^{-2}$
	σ_u	[-]	1.075	1.150 (*)
	β_a	[-]	1.114	1.278
	μ	[-]	$9.66*10^{-2}$	$22.70*10^{-2}$
Data	T_{wave}	[s]	8000	
	L_{river}	[m]	1000	
	Q_{min}	[m^3/s]	50.00	
	Q_{max}	[m^3/s]	150.00	
	M	[kg/s]	1.00	
	ϕ_0	[kg/m^3]	0.00	

(*) Equals the maximum value set for this parameter.

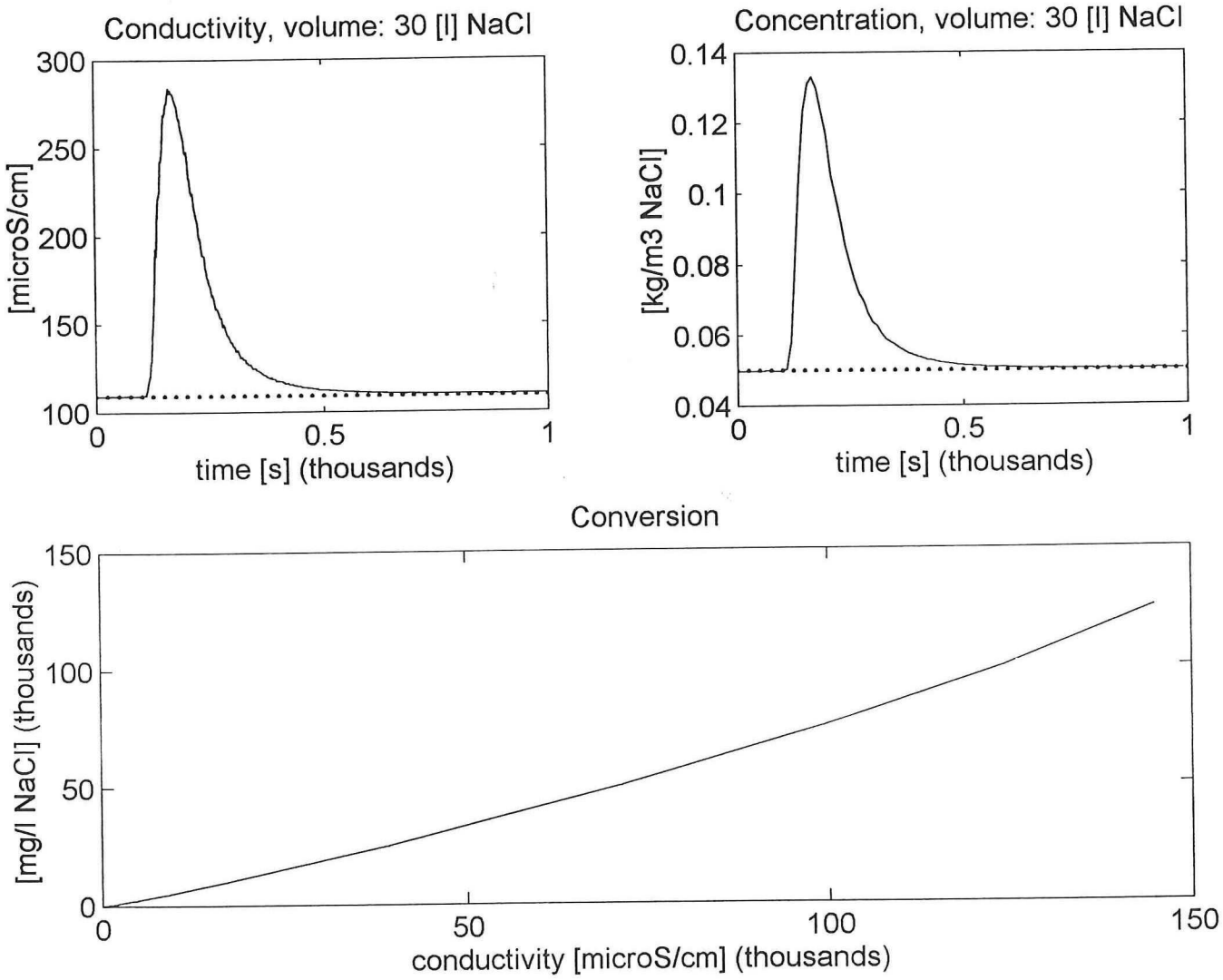
Conductivity, volume: 30 [l] NaCl
[microS/cm]
300
250
200
150
100
0
0.5
1
time [s] (thousands)
Concentration, volume: 30 [l] NaCl
[kg/m3 NaCl]
0.14
0.12
0.1
0.08
0.06
0.04
0
0.5
1
time [s] (thousands)
Conversion
[mg/l NaCl] (thousands)
150
100
50
0
0
50
100
150
conductivity [microS/cm] (thousands)

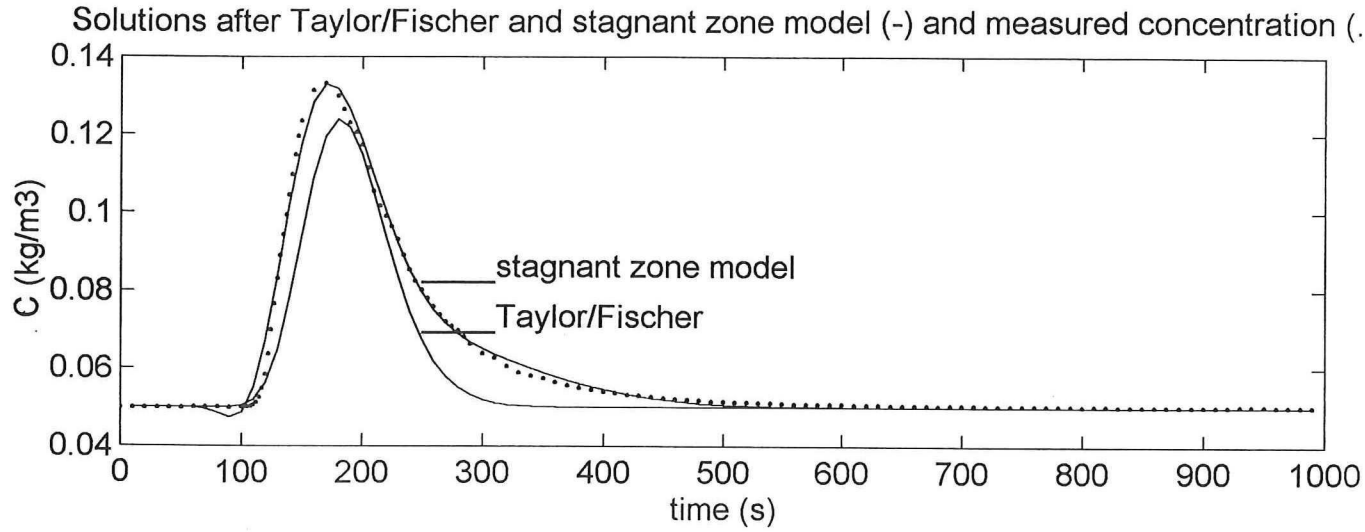
Solutions after Taylor/Fischer and stagnant zone model (-) and measured concentration (.)
C (kg/m3)
0.14
0.12
0.1
0.08
0.06
0.04
stagnant zone model
Taylor/Fischer
0
100
200
300
400
500
600
700
800
900
1000
time (s)

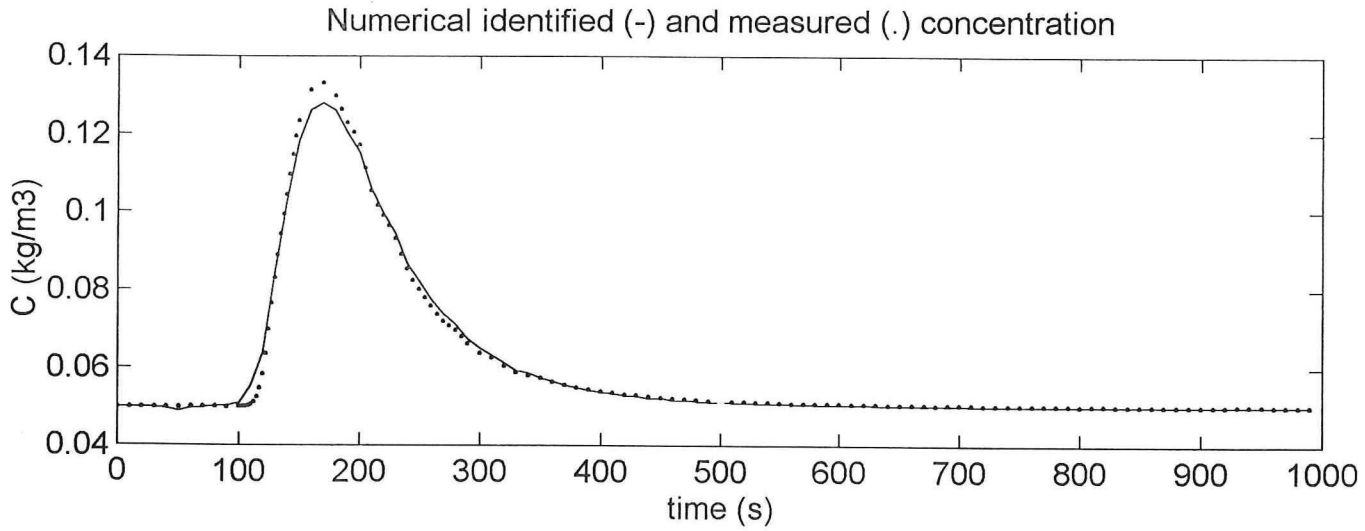
Numerical identified (-) and measured (.) concentration
C (kg/m3)
0.14
0.12
0.1
0.08
0.06
0.04
0
100
200
300
400
500
600
700
800
900
1000
time (s)

Numerical and analytical identified geometry

Schedule Ch.7		NUMERICAL:	ANALYTICAL:
Geometry	B_{up} [m]	2.817	2.800
	B_{down} [m]	4.196	2.800
	i_b [-]	$4.837*10^{-4}$	$1.720*10^{-5}$ (*)
	C [$m^{1/2}/s$]	19.95	30
	a [m]	0.605	1.70
Hydraulic	E [-]	$5.980*10^{-3}$	0.170
	f [-]	$1.629*10^{-2}$	1 (**)
	β_a [-]	1.123	n.a.
	μ [-]	$1.547*10^{-2}$	$1.200*10^{-2}$
Skewness:	G_t [-]	n.a.	1.000
Stagnant zone:	β_s [-]	1.6 %	2.7 %
Steady discharge:	Q_s [m^3/s]	0.582	0.765
Data:	L_{river} [m]	30	30
	M [kg]	3	3
	ϕ_0 [kg/m^3]	0.05	0.05

(*) Based on the Chézy-formula. The flow velocity u was computed as 0.163 [m/s]
(**) Overall presence.

The numerical identified value for σ_u is rewritten into a value for the stagnant zone coefficient β_s.